

Modelling of a Variable Venturi in a Heavy Duty Diesel Engine

Master's thesis
performed in **Vehicular Systems**

by
Carl-Adam Torbjörnsson

Reg nr: LiTH-ISY-EX-3368-2002

18th December 2002

Modelling of a Variable Venturi in a Heavy Duty Diesel Engine

Master's thesis

performed in **Vehicular Systems,**
Dept. of Electrical Engineering
at **Linköpings universitet**

by **Carl-Adam Torbjörnsson**

Reg nr: LiTH-ISY-EX-3368-2002

Supervisor: **Mattias Nyberg, PhD**
SCANIA CV
Jonas Biteus, MSc
Linköpings Universitet

Examiner: **Professor Lars Nielsen**
Linköpings Universitet

Linköping, 18th December 2002

	Avdelning, Institution Division, Department Vehicular Systems, Dept. of Electrical Engineering 581 83 Linköping	Datum Date 18th December 2002
	Språk Language <input type="checkbox"/> Svenska/Swedish <input checked="" type="checkbox"/> Engelska/English <input type="checkbox"/> _____	Rapporttyp Report category <input type="checkbox"/> Licentiatavhandling <input checked="" type="checkbox"/> Examensarbete <input type="checkbox"/> C-uppsats <input type="checkbox"/> D-uppsats <input type="checkbox"/> Övrig rapport <input type="checkbox"/> _____
URL för elektronisk version http://www.vehicular.isy.liu.se http://www.ep.liu.se/exjobb/isy/2002/3368/		
Titel Modellering av variabel venturi i en dieselmotor för tung lastbil Title Modelling of a Variable Venturi in a Heavy Duty Diesel Engine Författare Carl-Adam Torbjörnsson Author		
Sammanfattning Abstract <p>The objectives in this thesis are to present a model of a variable venturi in an exhaust gas recirculation (EGR) system located in a heavy duty diesel engine. A new legislation called EURO 4 will come into force in 2005 which affects truck development and it will require an On-Board Diagnostic system in the truck. If model based diagnostic systems are to be used, one of the advantages is that the system performance will increase if a model of a variable venturi is used.</p> <p>Three models with different complexity are compared in ten different experiments. The experiments are performed in a steady flow rig at different percentage of EGR gases and venturi areas. The model predicts the mass flow through the venturi. The results show that the first model with fewer simplifications performs better and has fewer errors than the other two models. The simplifications that differ between the models are initial velocity before the venturi and the assumption of incompressible flow.</p> <p>The model that shows the best result is not proposed by known literature in this area of knowledge and technology. This thesis shows that further studies and work on this model, the model with fewer simplifications, can be advantageous.</p>		
Nyckelord Exhaust gas recirculation, On-board Diagnostic, Flow meter, Model Keywords Based Diagnostic, Restriction, Compressible, Incompressible		

Abstract

The objectives in this thesis are to present a model of a variable venturi in an exhaust gas recirculation (EGR) system located in a heavy duty diesel engine. A new legislation called EURO 4 will come into force in 2005 which affects truck development and it will require an On-Board Diagnostic system in the truck. If model based diagnostic systems are to be used, one of the advantages is that the system performance will increase if a model of a variable venturi is used.

Three models with different complexity are compared in ten different experiments. The experiments are performed in a steady flow rig at different percentage of EGR gases and venturi areas. The model predicts the mass flow through the venturi. The results show that the first model with fewer simplifications performs better and has fewer errors than the other two models. The simplifications that differ between the models are initial velocity before the venturi and the assumption of incompressible flow.

The model that shows the best result is not proposed by known literature in this area of knowledge and technology. This thesis shows that further studies and work on this model, the model with fewer simplifications, can be advantageous.

Keywords: Exhaust gas recirculation, On-board Diagnostic, Flow meter, Model Based Diagnostic, Restriction, Compressible, Incompressible

Acknowledgment

This thesis has been done on a commission from Scania CV, Södertälje. I would like to thank the people at the department of Software and Diagnostics, Engine Control Systems who made my stay very pleasant. Special thanks go to Mattias Nyberg, Olof Lundström and Mikael Andersson at NMCS and Henrik Höglund and Jörgen Mårdberg at NMEE which help I could not have been without. At Vehicular Systems, Linköpings universitet a special thanks goes to my examiner Lars Nielsen and my supervisor Jonas Biteus.

Linköping, December 2002
Carl-Adam Torbjörnsson

Contents

Abstract	v
Preface and Acknowledgment	vi
1 Introduction	1
1.1 Background	1
1.1.1 EURO 4	1
1.1.2 Heavy duty diesel engine	2
1.1.3 Exhaust gas recirculation engine	3
1.2 Objectives	3
1.3 Target group	4
1.4 Delimitation	5
1.5 Methods	5
1.6 Methods criticism	5
1.7 Reader's guide	5
2 Exhaust gas recirculation models	6
2.1 Venturi	7
2.1.1 Variable venturi	8
2.2 General equations	9
2.3 Venturi model 1	11
2.4 Venturi model 2	13
2.5 Venturi model 3	13
3 Experiment	15
3.1 Percent exhaust gas recirculation	15
3.2 Collecting data	20
3.2.1 Pressure and temperature sensor	20
3.2.2 Mass flow sensor	21
3.3 Translate data	22
3.4 Air velocity	22

4	Results	24
4.1	Model fitting	24
4.1.1	Venturi model 1	26
4.1.2	Venturi model 2	26
4.1.3	Venturi model 3	27
4.2	Residual results	28
4.3	Air velocity	31
4.4	Discussion	31
4.4.1	Venturi model 1	32
4.4.2	Venturi model 2	33
4.4.3	Venturi model 3	33
4.4.4	Residual results	33
4.4.5	Discharge coefficient	34
5	Conclusions and extensions	35
5.1	Conclusions	35
5.2	Extensions	36
	References	37
	Notation	39
A	Equations	40
A.1	General equations	40
A.2	Derivations	40
B	Results	42
B.1	Velocities through the venturi	42
B.2	Venturi model 1	45
B.3	Venturi model 2	50
B.4	Venturi model 3	55

Chapter 1

Introduction

This thesis attempts to solve the problem of modelling the mass flow of an Exhaust Gas Recirculation (EGR) system. The problem is solved on a commission from Scania CV and within the final project and master's thesis made at Scania Södertälje, and at the division of Vehicular Systems at Linköpings universitet. In this chapter the objective, specification and background of this master's thesis are discussed.

1.1 Background

Scania was founded in 1891 and is today one of the world's leading manufacturers of heavy trucks and buses. Scania is an international corporation with operations in more than 100 countries. Ninety-seven percent of its production is sold outside Sweden. [1]

The trucks are developed, manufactured and sold with diesel engines due to the enhanced efficiency of a diesel engine compared to, for example, a petrol engine. Although the emissions today are higher with a diesel engine than other engines, there are several ways of reducing the diesel engine emissions.

1.1.1 EURO 4

In October 2005 a new legislation called EURO 4 will come into force that affects truck development. This will include limits for exhaust gas emission on Heavy Duty Diesel (HDD) vehicles. The legislator in Europe is the European Union and in the USA, the Environmental Protection Agency (EPA). The EU sets limits in Europe with EURO legislations.

EURO 4 limits for oxides of nitrogen (NO_x) is 3.5 g/kWh and for PM (particulate matter) it is 0.02 g/kWh , compared to EURO 3

limits of 5.0 g/kWh for NO_x and 0.1 g/kWh of PM emissions. The next legislation, EURO 5 will have even tougher specification limits. However, these limits have not yet been determined. EURO 4 will also require an On-Board Diagnostic (OBD) system. When there is a risk that an error on the truck will lead to increased emission, the driver will be warned by the system. One way of alerting the driver is a warning light on the dashboard.

A possible way of creating this OBD system is through Model Based Diagnostic. By using a model of the engine parallel with the engine sharing the same input¹ and output² signals. When the model of the engine and the real engine differ and there is a risk of increased emission, the driver will be notified. The incident will also be recorded in a logging device of the engine.

1.1.2 Heavy duty diesel engine

A diesel engine and a petrol engine differs more than just the fuel used to run the engine. Most cars today run with a four stroke spark ignited petrol engine. Heavy trucks runs on diesel engines mostly due to their higher efficiency. The main differences between the petrol engine and the diesel engine are:

Ignition A petrol engine intakes a mixture of gas and air, compresses it and ignites the mixture with a spark. A diesel engine takes in just air, compresses it and then injects fuel into the compressed air. The heat of the compressed air lights the fuel spontaneously.

Pressurization A petrol engine compresses at a ratio of 8:1 to 12:1, while a diesel engine compresses at a ratio of 14:1 to as high as 25:1. The higher compression ratio of the diesel engine the better efficiency.

Feeding of fuel A petrol engine generally uses either carburetion, in which the air and fuel is mixed long before the air enters the cylinder, or port fuel injection, in which the fuel is injected just prior to the intake stroke (outside the cylinder). Diesel engines use direct fuel injection, the diesel fuel is injected directly into the cylinder.

Another difference between diesel engines and petrol engines is in the injection process. Most car engines use port injection or a carburetor rather than direct injection. Therefore, in a car engine, all of

¹Examples of input signals are: Throttle, intake air temperature, engine temperature, amount air flowing into the engine and signal from lambda sensor.

²Examples of output signals are: Engines torque, emissions such as NO_x and PM, fuel consumption and voltage from the generator.

the fuel is loaded into the cylinder during the intake stroke and then compressed. The compression of the mixture of gas and air limits the compression ratio of the engine. If it compresses the air too much, the mixture of gas and air spontaneously ignites and causes knocking. A diesel compresses only air, so the compression ratio can be much higher. The higher the compression ratio, the more power is generated. Therefore the higher efficiency. [2]

1.1.3 Exhaust gas recirculation engine

Oxygen is required for fuel to burn in an engine. This is usually supplied by taking in air from the atmosphere. The high temperatures found within the engine cause nitrogen to react with oxygen to form NO_x .

The burned gases act as a diluent in the unburned mixture; the absolute temperature reached after combustion varies inversely with the burned gas mass fraction. Hence increasing the burned gas fraction reduces NO emissions levels.

Addition of diluents [exhaust gas (EGR) and nitrogen] reduce peak flame temperatures and NO_x emissions; also, addition of oxygen (which corresponds to a *reduction* in diluent fraction) increase flame temperatures and therefore increase NO_x emissions.

Diluents added to the intake air (such as recycled exhaust) are effective at reducing the NO formation rate, and therefore NO_x exhaust emissions. [3]

NO_x are one of the main pollutants emitted by vehicle engines and are legislated by EURO 4. One way to control NO_x is to use EGR. This technique directs some of the exhaust gases back into the intake of the engine to dilute the fresh air.

There is one small problem with EGR though. In a worst case scenario, at low engine load and speed, the pressure difference between the exhaust and the inlet of the engine could level out, or even worse, could lead to a negative pressure drop and the EGR gases would not flow towards the inlet manifold. Figure 1.1 identifies the name of the different pressures and the alignment of an EGR system on a HDD engine. To move low pressured gas to a high pressured chamber without losing too much efficiency is difficult. How this problem affects the EGR and is solved is explained in Chapter 2.

1.2 Objectives

In order to satisfy EURO 4, an OBD system is needed and lower NO_x emissions are required. An EGR-system lowers NO_x emissions, and if

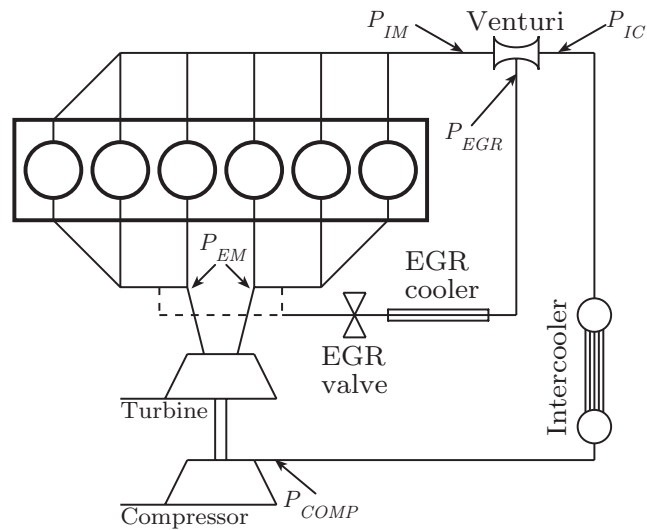


Figure 1.1: Sketch of a turbo charged engine with EGR.

EGR is used the EGR must be diagnosed and modelled.

The venturi is one way of making the EGR work. To make the EGR model function, and to be able to diagnose the venturi, the venturi should be modelled.

The objectives of this thesis are to present a model of a variable venturi that can be used to model the mass flow through the EGR. Thereafter, verify how the same model models the mass flow through the whole variable venturi.

1.3 Target group

The target groups of this thesis are the people working at Scania CV, undergraduate students, graduate students and others at the division of Vehicular Systems at Linköpings universitet. Even others that have some knowledge and interest of fluid dynamics, diagnosis and engines may have interest of this.

To fully understand the theory and results presented, common knowledge of diesel and petrol engines, fluid dynamics, control theory and diagnosis are required.

1.4 Delimitation

Data needed to solve the problem are collected when needed from experiments performed with existing equipment. Only one venturi is used during measurements.

1.5 Methods

The methods are based on literature studies and experiments.

To find literature that makes enough assumptions to help solve the problem in this case, before the results are available and evaluated, is difficult and therefore iterative problem solving is used. Recommendations made by the authors and other specialists in this subject area are considered. Experiments are of qualitative characteristic and based on observations and data collecting sessions with available equipment.

1.6 Methods criticism

One problem with fluid dynamics is that there is no exact analytic solution without any assumptions made, it is simply too complicated. [4] That said, the task is to solve the problem with enough assumptions, so the problem can be solved in an analytical way without becoming inaccurate.

Books were used to collect theory, which mainly is used in education at undergraduate courses. The books used were recommended by professors and experts and is a small part of the existing literature.

The use of not optimal experiment equipment, not calibrated sensors or a controlled environment where the experiments took place can worsen the model and the results. Temperature, pressure and mass flow of air or mass flow of EGR gases could not reach real values as in a real running engine.

1.7 Reader's guide

Chapters follow a logical order of designing a model of an EGR, in a chronological order. Create the model with equations first, Chapter 2, to be able to pick which variable to measure. Then, measure and collect data of different parts of the EGR system, Chapter 3. Verify the model with experiments data, Chapter 4 and analyze the result. Finally a discussion, Section 4.4 before Chapter 5 rounds up this thesis with a conclusion and extension.

Chapter 2

Exhaust gas recirculation models

This chapter includes the theory of exhaust gas recirculation and more precise the theory of the variable venturi. It also includes how EGR function, where EGR is introduced on an engine and how to model the critical part of the EGR, the variable venturi.

As explained in Section 1.1.2 there is a problem with EGR systems. The problem is not the system itself but the characteristic of the engine it is mounted upon. If EGR system is introduced on an engine there are several things and parts which must be considered. The most evident characteristic of a turbo charged HDD engine is the magnitude of its different pressures through out the engine. For an example, after the turbo has compressed the air and the intercooler has cooled down the air and lowered the pressure the air still has about 3 bar mean value of pressure at full load. To reach highest possible efficiency all of the pressure from the combustion should be used to accelerate the piston. That means the pressure should be near ambient pressure, about 1 bar , when leaving the combustion chamber to the exhaust manifold. However, in reality the pressure is still high and the rest of the gas energy is used to spin the turbine so the compressor can compress the air at the intake side of the engine.

The main task for EGR system is, as told before, to lower NO_x emissions. Therefore, the EGR has to somehow move an amount of the burned gas from the low pressure in the exhaust manifold to the high pressure inlet manifold. But as gas flows from high pressure to low pressure if no work is done on the gas. As there is a much higher mean value pressure in the inlet manifold then in the exhaust manifold the net flow would be flowing the wrong way, from the inlet manifold to the exhaust manifold and that would lower the efficiency of the engine.

The engine might even stop working properly.

There are two possibilities to make EGR function. Either work on the gas, for an example a compressor or some kind of a pump would do the work on the gas to raise the gas pressure. If the pressure is raised then the gas could flow towards the inlet manifold. Secondly lower the pressure on the air in the inlet manifold to allow the burned gases from the exhaust manifold flow towards a lower pressure. As always all losses must be reduced. The first idea of work on the gas would further make the system more complex and therefore the first possibility is rejected.

To maintain a positive flow of gases from exhaust manifold to inlet manifold the pressure difference $P_{EM} - P_{IM}$ in Figure 1.1 must be positive. There are two common ways of doing this:

1. Introduce a throttle between the intercooler and the intake. With a throttle it is easy to control the pressure difference $P_{EM} - P_{IM}$ but with a huge impact on the efficiency due to the low pressure of air before combustion.
2. Use a venturi pipe between the intercooler and the inlet manifold. Due to the venturi's characteristic there will be a *local* lowering of the pressure at the venturi throat. Where the pressure is lowered the EGR gases should be lead into the venturi.

As explained earlier, higher pressure of air before combustion leads to higher efficiency which means a lowering of the pressure is out of the question. The venturi pipe would only lower the pressure at a small section to allow the EGR gas to dilute the fresh air before the inlet and therefore is the better choice.

2.1 Venturi

The main difference between a throttle and a venturi is that the venturi has a diffuser after the venturi throat. This does not change the equation used as will be shown. However, this is easy realized when the same equations is used to derive the throttle, the venturi and the nozzle. The main differences between the equations of a throttle and a venturi are constants which depends on geometry. The nozzle is calculated as a restriction. The diffusers main task is to raise the pressure to what it was before the restriction.

In Figure 2.1 the intersection * can be placed anywhere between section 0 and * but is placed at the venturi throat where the area is smallest.

If the venturi is to be seen as two parts, from left to right in Figure 2.1, one converging part called a restriction or nozzle and one diverging part called a diffuser. The two parts connects at the narrow

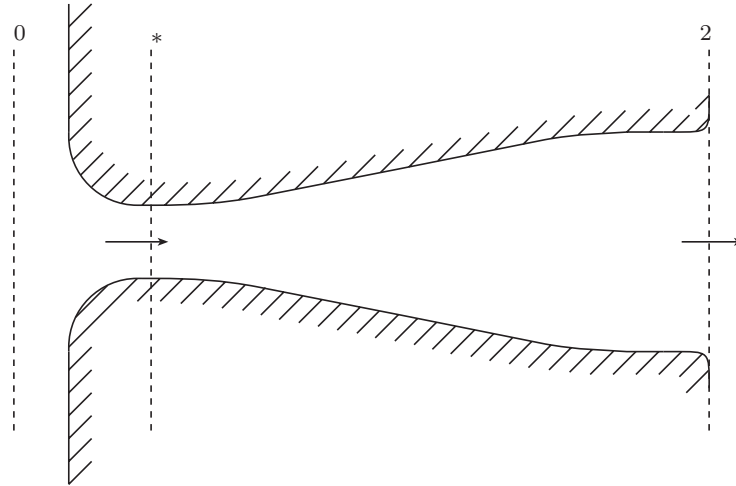


Figure 2.1: Split view of a schematic venturi. The intersection of index * is placed at an arbitrary position between indexes 0 and 2.

part, a throat called section *. This passage is often called a critical passage due to the possibility to accelerate air to super sonic speeds when passing through the venturi throat.

2.1.1 Variable venturi

The forming of NO_x during combustion is complex. How the venturi is designed affects both the engine's efficiency and emissions. Two important aspects are:

- At low engine speeds a higher percentage of EGR is required to lower NO_x emissions than at high engine speeds.
- The pressure loss in the venturi is increasing with smaller area at the throat. At high engine speeds the air flows faster through the venturi and the pressure loss is increasing with greater air velocities.

Thus at high air velocities no restriction, or smaller area, in the air stream is wanted or required. An idea to solve this problem is use of a variable restriction. That means the area of the *local* restriction could be changed. The idea is to change the critical area of the venturi, the venturi throat. If a *wedge* was to be inserted in the critical section without interfere with the flow of air on any other way, primary than

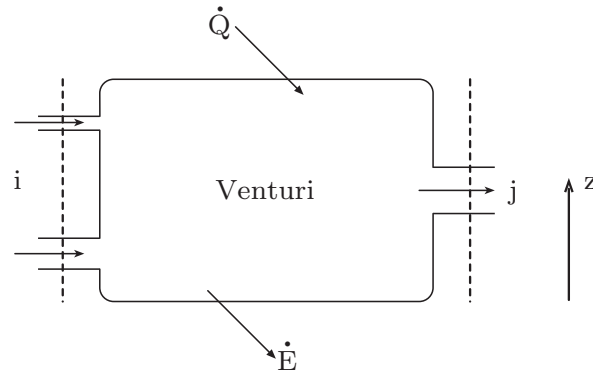


Figure 2.2: System view of the energy in a venturi.

making the area smaller, the design problem is solved. The designing of a model of a variable venturi would also need to be a function of the area of the variable restriction.

Even though the venturi to be modelled is a variable venturi it will be called a venturi due to the fact that the only difference is the area change under some circumstances.

2.2 General equations

The system of the venturi is defined as an open system. That is an imaginary system surrounding and containing the venturi with a boundary that lets media flow in and out of the system.

The derivation of the three different models all start from the same energy equation only some assumptions differs in the different models. The energy equation defined in a system, shown in Figure 2.2, has two inlet and one exhaust. The general energy equation of that system is in every stationary case

$$\dot{Q} = \dot{E} + \sum_j \dot{m}_j \left(h_j + \frac{w_j^2}{2} + gz_j \right) - \sum_i \dot{m}_i \left(h_i + \frac{w_i^2}{2} + gz_i \right)$$

where

$$\begin{aligned}\dot{Q} &= \text{heat transfer [J/s]} \\ \dot{E} &= \text{rate of energy transfer as work [W]} \\ \dot{m} &= \text{mass flow rate [kg/s]} \\ h &= \text{enthalpy [J/kg]} \\ w &= \text{velocity [m/s]} \\ g &= \text{the gravitational acceleration [m/s}^2\text{]} \\ z &= \text{height to inlet or exhaust [m].}\end{aligned}$$

One assumption made this early is that there is little differences in height between the inlet and the outlet. The product $g\Delta z \approx 0$. Also the mass flow of the EGR, the smaller inlet pipe into the system is assumed to be very small compared to the total mass flow through the venturi. Therefore the energy equation is, when divided with the mass flow of the system, when using indexes 0 for inlet and 2 for the exhaust,

$$q = \varepsilon + \left(h_2 + \frac{w_2^2}{2} \right) - \left(h_0 + \frac{w_0^2}{2} \right), \quad (2.1)$$

where ε is the work done by the system or put into the system and is zero in this case. No heat is exchanged between the system and the surrounding, i.e. *adiabatic*. Hence, the heat transfer of the system is assumed to be zero, $q = 0$.

The Figure 2.1 shows the schematic view of a venturi with only one inlet and one exhaust with the new indexes which is used to derive the rest of the equations. At each intersection in the figure the venturi has a given area and the air passing through has a given velocity, temperature, pressure and mass flow. Equation (2.1) is rewritten to apply from section 0 to arbitrary section *

$$w_*^2 - w_0^2 = 2(h_0 - h_*). \quad (2.2)$$

Other general assumptions are:

All gas is concerned as an *ideal gas*. Thus the ideal gas law applies, $p\nu = RT$, where the density is $\rho = \frac{1}{\nu}$ and ν is specific volume [m^3/kg].

The process is assumed to be *adiabatic* and *reversible*¹ i.e. *isentropic*, and $pv^\kappa = \text{const.}$

¹If a process can be made to reverse itself completely in all details and follows the exact same path it originally followed, then it is said to be *reversible* [5].

The law of conservation of mass is

$$\dot{m} = \rho w A \quad (2.3)$$

and is constant through the venturi due to constant mass flow. Also this is assumed due to the fact that the same amount air entering into the engine, seen from intercooler in Figure 1.1, will also leave the engine seen from the compressor if the engine has not got a leakage.

In many parts of the engine cycle, fluid flows through a restriction or reduction in flow area. Real flows of this nature are usually related to an equivalent ideal flow. The equivalent ideal flow is the steady adiabatic reversible flow of an ideal fluid through a duct of identical geometry and dimensions. For a real fluid flow, the departures from the ideal assumptions listed above are taken into account by introducing a flow coefficient or discharge coefficient C_D , where

$$C_D = \frac{\text{actual mass flow}}{\text{ideal mass flow}}.$$

The discharge coefficient together with (2.3) is actual mass flow

$$\dot{m} = C_D \rho w A. \quad (2.4)$$

With ideal gas, the entropy is a function of only temperature. c_p is also only a function of temperature and with indexes from Figure 2.1

$$h_0 - h_* = c_p (T_0 - T_*) \quad (2.5)$$

where

$$c_p = \frac{\kappa R}{\kappa - 1}. \quad (2.6)$$

These equations applies for all models and with additional simplifications three models are to be designed. General derivations used in the next sections is found in Appendix A.

2.3 Venturi model 1

Energy equation right hand side (2.2) together with (2.5) and (2.6)

$$2(h_0 - h_*) = \frac{2\kappa R}{\kappa - 1} (T_0 - T_*) = \frac{2\kappa R T_0}{\kappa - 1} \left(1 - \frac{T_*}{T_0}\right) \quad (2.7)$$

and with assumption of ideal gas and isentropic process

$$\frac{T_*}{T_0} = \Pi^{\frac{\kappa-1}{\kappa}} \text{ where } \Pi = \frac{p_*}{p_0}, \quad (\text{A.11}) \quad (2.8)$$

the right hand side are

$$\frac{2\kappa RT_0}{\kappa - 1} \left(1 - \Pi^{\frac{\kappa-1}{\kappa}}\right). \quad (2.9)$$

The law of conservation, (2.3) with indexes 0, *

$$\dot{m} = \rho_0 w_0 A_0 = \rho_* w_* A_* \quad (2.10)$$

and solve for w_0

$$w_0 = w_* \frac{\rho_* A_*}{\rho_0 A_0}$$

the left hand side of (2.2) is

$$w_*^2 \left(1 - \left(\frac{\rho_* A_*}{\rho_0 A_0}\right)^2\right) = w_*^2 - w_0^2. \quad (2.11)$$

Finally calculate the mass flow at the intake in the venturi. Equation (2.2), (2.9) and (2.11)

$$w_*^2 \left(1 - \left(\frac{\rho_* A_*}{\rho_0 A_0}\right)^2\right) = \frac{2\kappa RT_0}{\kappa - 1} \left(1 - \Pi^{\frac{\kappa-1}{\kappa}}\right)$$

and solve for w_* when $\frac{\rho_*}{\rho_0} = \left(\frac{p_*}{p_0}\right)^{\frac{1}{\kappa}} = \Pi^{\frac{1}{\kappa}}$

$$w_* = \sqrt{RT_0} \sqrt{\frac{\frac{2\kappa}{\kappa-1} \left(1 - \Pi^{\frac{\kappa-1}{\kappa}}\right)}{1 - \Pi^{\frac{2}{\kappa}} \left(\frac{A_*}{A_0}\right)^2}}$$

Finally, when

$$\rho_* = \Pi^{\frac{1}{\kappa}} \frac{p_0}{RT_0}$$

the actual mass flow of air at the section * is

$$\dot{m} = C_D \rho_* w_* A_* = \frac{C_D A_* p_0}{\sqrt{RT_0}} \frac{\Psi(\Pi)}{\sqrt{1 - \Pi^{\frac{2}{\kappa}} \left(\frac{A_*}{A_0}\right)^2}} \quad (2.12)$$

$$\Psi(\Pi) = \sqrt{\frac{2\kappa}{\kappa-1} \left(\Pi^{\frac{2}{\kappa}} - \Pi^{\frac{\kappa+1}{\kappa}}\right)}$$

which is called *venturi model one* and later used to estimate or simulate the mass flow of air through the venturi.

The simplification made for model 1 is

- The flow is one dimensional.
- The mass flow of EGR is small and therefore neglected.
- Ideal gas law applies.
- The process is isentropic and adiabatic.

2.4 Venturi model 2

Model 2 is recommended by [3] to use when modelling a venturi. To derive model two, assume that the volume before the venturi throat, section 0 in Figure 2.1 is big therefor the speed w_0 is close to zero and neglected.

The right hand side in (2.2) is as derived in Section 2.3. The left hand side is the velocity of air in arbitrary section $*$ and is w_*^2 . The actual mass flow of air at the section $*$ is

$$\begin{aligned} \dot{m} &= C_D A_* \rho_* w_* = \frac{C_D A_* p_0}{\sqrt{RT_0}} \Psi(\Pi) \\ \Psi(\Pi) &= \sqrt{\frac{2\kappa}{\kappa-1} \left(\Pi^{\frac{2}{\kappa}} - \Pi^{\frac{\kappa+1}{\kappa}} \right)} \end{aligned} \quad (2.13)$$

The simplification made for model 2 is

- The flow is one dimensional.
- The mass flow of EGR is small and therefore neglected.
- Ideal gas law applies.
- The process is isentropic and adiabatic.
- The velocity of air before the venturi is neglected.

2.5 Venturi model 3

Assume the velocity of air through the venturi is low and therefor the air is incompressible and density is constant. $\rho_0 = \rho_*$ or equally the specific volume is constant $v_0 = v_*$. To derive model 3, start from (2.2). Assume the volume before the venturi, index 0 in Figure 2.1 to be big therefore the velocity of the medium close to zero and neglect the coefficient of w_0 . As before the speed at section $*$ is

$$w_* = \sqrt{2(h_0 - h_*)}.$$

Finally solve for the actual mass flow at section $*$ with (2.4), (2.5), (2.6) and ideal gas law, $T = \frac{pv}{R}$ is

$$\dot{m} = \frac{C_D A_* \sqrt{p_0}}{\sqrt{RT_0}} \sqrt{\frac{2\kappa}{\kappa-1} (p_0 - p_*)} \quad (2.14)$$

The simplification made for model 3 is

- The flow is one dimensional.

- The mass flow of EGR is small and therefore neglected.
- Ideal gas law applies.
- The process is isentropic and adiabatic.
- The velocity of air before the venturi is neglected.
- Assume incompressible flow.

Chapter 3

Experiment

Experiments will be performed with existing equipment. This means settle with gathered data. For example, none shielded cable, use of not calibrated sensors and ambient temperature and pressure vary over time. All this sum up to a signal which require a lot of work to extract the information from, that is required to model the variable venturi.

A steady flow rig is the existing laboratory equipment available. Since this rig is used, correct air mass flow through the venturi may be difficult to achieve because the use of an air pump instead of an air compressor¹. Figure 3.1 and Figure 3.2 illustrates the differences between the steady flow rigs maximum mass flow and the mass flow in an engine with compressor. Air will flow the correct way and the same direction but with less pressure and less mass of air. About one third of the air mass flow in the engine bench is achieved with the steady flow rig. [6] If correct air velocity is achieved, higher mass flow in the engine bench leads to higher density. However it is assumed that not using correct air mass flow does not affect the result of modelling the EGR to much.

More important is to achieve velocity corresponding to air velocities in the real EGR since it is likely that air velocity is high and close to sound velocity. As a rule of thumb air velocity more then Mach 0.3 is considered compressible and close to sound velocity. [5] Due to characteristic of gases the velocity is more critic then air mass flow and affect the EGR model more.

3.1 Percent exhaust gas recirculation

Ten different experiments created with five different settings on the variable restriction at EGR inlet and two settings on the venturi wedge.

¹In a HDD engine a compressor is used to feed the inlet of the engine with air.

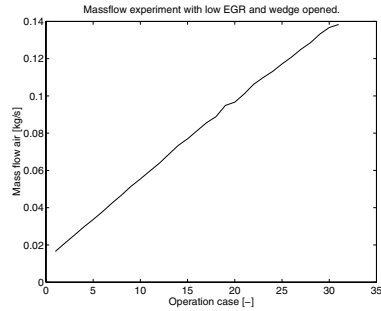


Figure 3.1: Mass flow of air through venturi in steady flow rig in experiment with low EGR and venturi wedge opened.

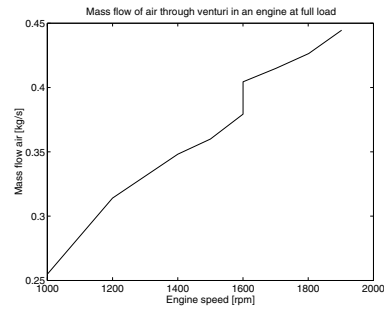


Figure 3.2: Mass flow of air through an engine with EGR-system and variable venturi in an engine bench at full load.

Table 3.1: Different levels percent of EGR in the operation cases.

Operation case name	Open wedge	Closed wedge
	Percent EGR of \dot{m}	Percent EGR of \dot{m}
Minimum	0	0
Low	0	0
Medium	6.8	12.9
High	20.5	37.1
Maximum	29.5	57.6

For closed venturi wedge a higher percentage of EGR was achieved. In the Table 3.1 the mean value of percent EGR through the venturi at different settings of the venturi wedge and the variable restriction shown in Figure 3.4 ‘Minimum EGR’, 3.5 ‘Low EGR’, 3.6 ‘Medium EGR’, 3.7 ‘High EGR’ and 3.8 ‘Maximum EGR’. The sensor air velocity through EGR in experiment with low EGR gave no output reading due to low sensibility but a pressure drop in EGR inlet was measured. Thus the calculations of percentage EGR for experiment low EGR is zero. As an example the experiment with maximum percentage EGR and with the venturi wedge opened the different operation cases estimates as 29.5% EGR, Figure 3.3.

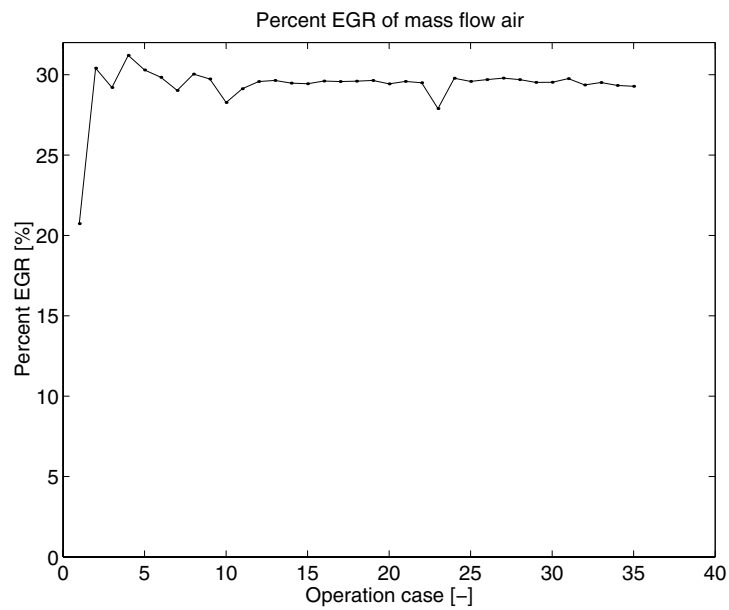


Figure 3.3: Percentage EGR at different operation cases in experiment with maximum EGR and venturi wedge opened. The result is estimated as a mean value of 29.5% EGR.



Figure 3.4: Picture of restriction position when doing EGR flow experiment, called minimum or no EGR.



Figure 3.5: Picture of restriction position when doing EGR flow experiment, low EGR.



Figure 3.6: Picture of restriction position when doing EGR flow experiment, medium EGR.



Figure 3.7: Picture of restriction position when doing EGR flow experiment, high EGR.



Figure 3.8: Picture of restriction position when doing EGR flow experiment, maximum EGR.

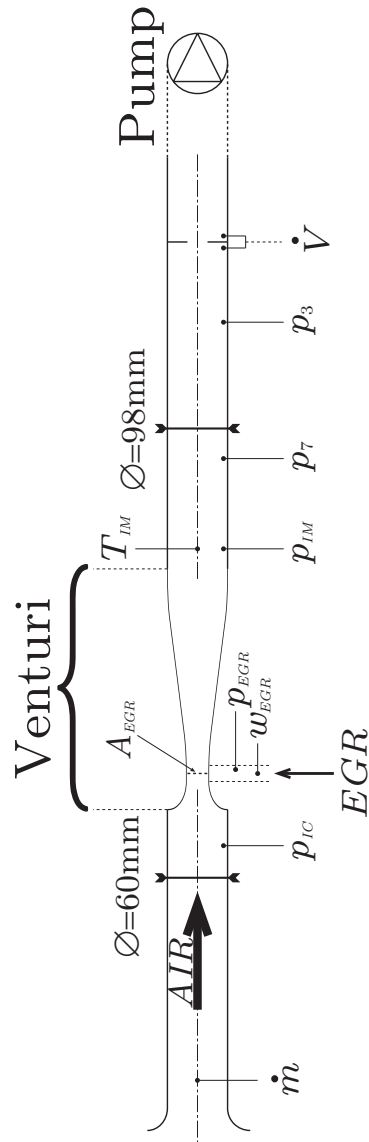


Figure 3.9: Schematic layout of experiment plant, the steady flow rig setup.

3.2 Collecting data

The setup of the experiment is shown in Figure 3.9 and the different channels are labelled from one to nine. The nine different quantities of the experiment is recorded during ten different series of data collection as explained in Section 3.1.

1. \dot{m} , Mass flow sensor.
2. \dot{V} , Volume flow.
3. P , Pressure, before volume flow sensor.
4. P_{EGR} , Pressure, after EGR cooler, before venturi.
5. P_{IM} , Pressure, in inlet manifold.
6. T_{IM} , Temperature, in inlet manifold.
7. P_7 , Pressure, after inlet manifold.
8. P_{IC} , Pressure after mass flow sensor.
9. v_{EGR} , Velocity of air through EGR after EGR cooler, before venturi.

To be able to create a model, the EGR mass flow, the mass flow before the venturi \dot{m} , the temperature before the venturi T_0 , the pressure before and the pressure in the critical section in the venturi are needed. The five remaining sensors were measured for redundancy and calibration.

3.2.1 Pressure and temperature sensor

As explained earlier in Chapter 2, pressure and temperature in inlet manifold is required to be able to estimate EGR mass flow. On the real engine, there is a sensor placed in the inlet manifold which is mounted on the end of the venturi's diffusor. Therefore, the same sensor mounted at the same place is measured during experiment to give some information about how it will behave when mounted in a real engine. To calculate the pressure in the inlet manifold an equation was given

$$U_{out} = \frac{U_{ref}}{5} \frac{1}{14} (16P - 1) \quad (3.1)$$

where U_{out} was measured and logged and $P_{IM} = P$. [7] U_{ref} was set at 5 volts.

The calibration of the final models from Chapter 2 depends on which pressure sensor is used. From Section 3.2 the two sensors P_7 and P_{IM}

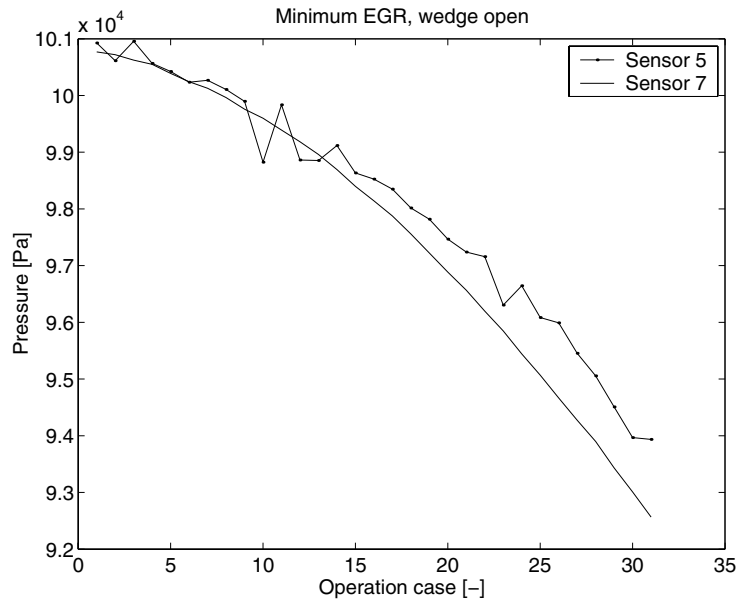


Figure 3.10: Sensors number five and sevens different characteristic. Pressure measured during experiment with minimum EGR and venturi wedge opened.

are plotted from one experiment, Figure 3.10. The pressure sensor number seven, P_7 , has a better characteristic than sensor number five, P_{TM} , and therefore sensor seven is used when modelling from section 0 to 2. This could be due to pressure sensor five voltage and current feeding from a questionable power supply source.

3.2.2 Mass flow sensor

The most critical sensor in the experiment is the mass flow sensor². Without the mass flow sensor no validation could be made. Also in a real engine running the diagnosis system a failure of the mass flow sensor is critical.

The mass flow sensor used in experiments have a range of 0 to 0.14 kg/s therefore no measuring was made higher than the maximum limit of the mass flow sensor.

²Mass flow sensor used in experiments in steady flow rig is a hot-film air-mass sensor, HFM2C. [8]

3.3 Translate data

Different *operation cases* were used to be able to repeat and reproduce the data collection. The mass flow through the venturi was controlled by a pump. When a sensor saturated, the experiment was aborted.

To collect and save sensor output voltage, a PC was used. For each operation case, 100 samples from all eight channels was saved with a sample time of 0.1 s. After an experiment was aborted a plot of all data looks like Figure 3.11.

- Remove five highest and lowest values of the 100 measured data in a operation case, calculate the mean value of the remaining data.
- For each operation case, remove the remaining data if a sensor is saturated.
- Calculate the absolute value in SI units.

Different sensors was saturated in different experiments due to different settings of the variable restriction in the inlet of EGR and the venturi wedge.

3.4 Air velocity

From Section 2.1 and the law of conservation of mass, (2.3) is $\dot{m} = \rho w A$ at the given section. The velocity is calculated at section indexed 0 before the venturi, the critical section index * and after the venturi index 2. The two different areas at the critical section are used to calculate the different velocities at that section. The smaller area when the venturi wedge is closed and thus the greater area when calculating opened venturi wedge.

Chapter 4

Results

This chapter will present the results of the experiments from the steady flow rig and how the models correspond to the measured data. Both from section 0 to * and 0 to 2. All result figures and tables from model fitting are listed in Appendix B.

4.1 Model fitting

The Figure 4.1 shows the result of model 1 approximating the mass flow with the pressure p_0 and p_* . The data from the experiment plotted is with medium EGR, approximately 13 percent, and the venturi wedge closed. The X-axis is the modelled mass flow and the Y-axis is the measured mass flow.

The Figure 4.2 shows the residual of the result in Figure 4.1. The fit residuals are defined as the difference between the ordinate data point and the resulting fit for each abscissa data point. The Table 4.1 is a summation of the coefficients, norm and standard deviation for experiment from section 0 to * with closed venturi wedge.

Table 4.1: Results of fittings. Model 1, section 0 to *.

Experiment	Coefficients, p1	Coefficients, p2	Norm of residuals	Standard deviation
Minimum closed	0.97117	0.00046634	0.0020747	0.385e-003
Low closed	0.98886	0.00038561	0.0026826	0.467e-003
Medium closed	0.99858	0.00054486	0.0033943	0.566e-003
High closed	1.0447	0.0030482	0.007653	1.154e-003
Maximum closed	2.9585	0.0021822	0.027442	4.639e-003

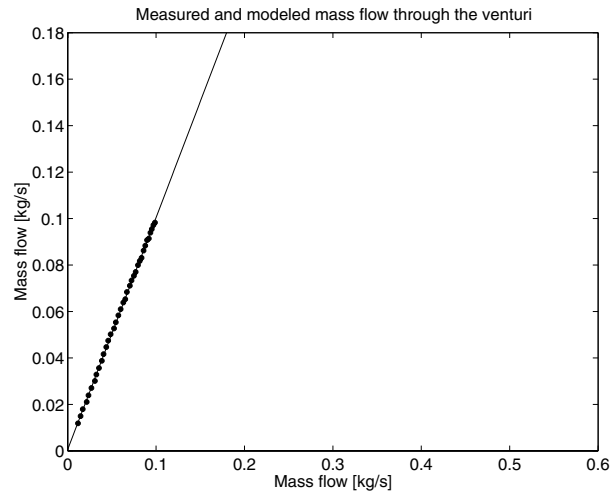


Figure 4.1: Result of model 1 from 0 to *, experiment medium EGR and closed wedge.

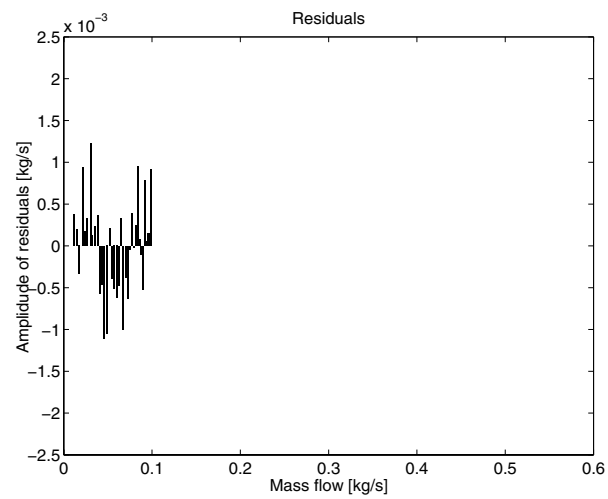


Figure 4.2: Residual of model 1 from 0 to *, experiment medium EGR and closed wedge.

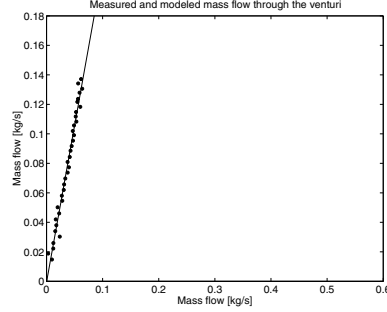


Figure 4.3: Model 1 from section 0 to * with maximum EGR and *opened* venturi wedge.

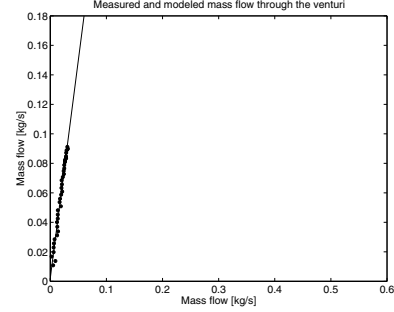


Figure 4.4: Model 1 from section 0 to * with maximum EGR and *closed* venturi wedge.

4.1.1 Venturi model 1

Model 1 uses (2.12) to model the mass flow. The model plotted against the measured data is estimated as a straight line corresponding to equation $y = p_1 * x + p_2$. For an example, the equation for the straight drawn line in Figure 4.1 is $y \approx x + 0.5 \times 10^{-3}$ and the coefficients can be found in Table 4.1. The one constant not fixed in the models is used to approximate the actual mass flow and is the discharge coefficient C_D . The discharge coefficient is equal with the coefficient p_1 in the tables. Steeper slope of the straight line in Figure 4.1 is a greater C_D and a greater resistance to the flow of air through the venturi. $\|r\|_2$ of the residual is also found in the same table and is 3.3943×10^{-3} . In the same table the standard deviation is calculated and is for the same experiment 0.566×10^{-3} . Lower $\|r\|_2$ and lower standard deviation is better fit of the straight line.

Figure 4.3 and Figure 4.4 illustrates the worst fit within the experiment. The experiment is with opened and closed venturi wedge with maximum EGR when modelling from section 0 to *. Standard deviation of the fit from experiment with opened wedge is $\|r\|_2 = 6.2 \times 10^{-3}$ and for the experiment with closed wedge it is $\|r\|_2 = 4.6 \times 10^{-3}$. What can be noticed in the figures are, the slope of the straight lines are not equal.

4.1.2 Venturi model 2

Model 2 differs from previous model with one assumption. The initial velocity of air before entering the variable venturi is assumed to be zero and neglected.

The two Figures 4.5 and 4.6 illustrates the worse fit with opened and closed venturi wedge. Maximum EGR in experiment when modelling

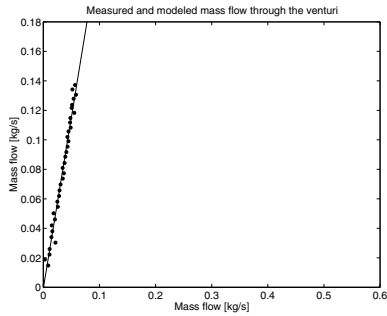


Figure 4.5: Model 2 from section 0 to * with maximum EGR and *opened* venturi wedge.

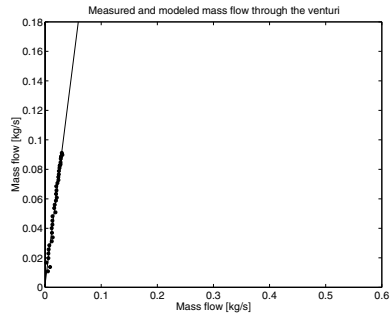


Figure 4.6: Model 2 from section 0 to * with maximum EGR and *closed* venturi wedge.

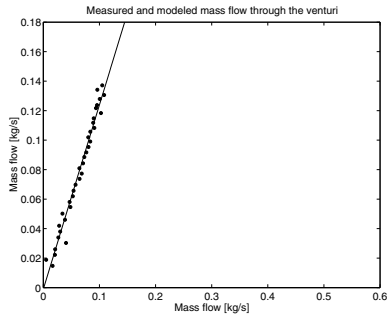


Figure 4.7: Model 3 from section 0 to * with maximum EGR and *opened* venturi wedge.

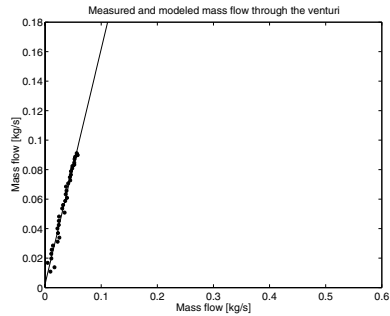


Figure 4.8: Model 3 from section 0 to * with maximum EGR and *closed* venturi wedge.

from section 0 to *.

Similar characteristic between the different experiments as in model 1 can be noticed for model 2. The slope differs if the wedge is opened or closed and differs if the percentage EGR changes.

4.1.3 Venturi model 3

Model 3 differs from model 2 and therefore also differs from model 1. The difference between model 2 and model 3 is that in model 3 assumes the air flow to be incompressible. Figure 4.7 and 4.8 illustrates the worse fit with opened and closed venturi wedge. Maximum EGR in experiment when modelling from section 0 to *. The slope of the straight lines in the figures are almost the same.

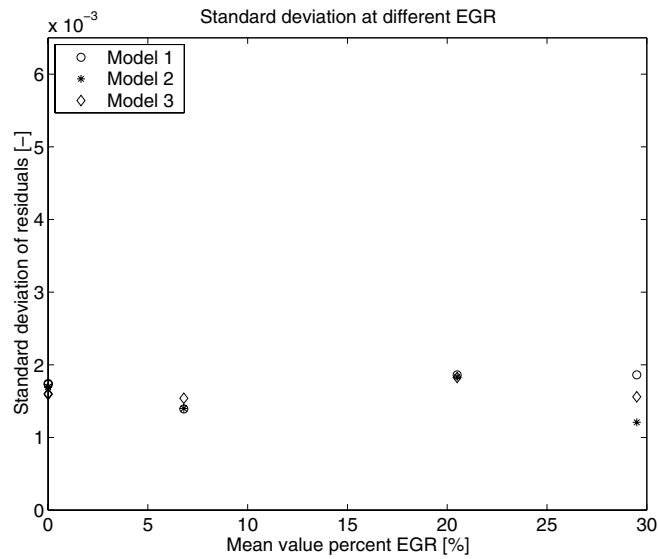


Figure 4.9: Standard deviation of the residuals from experiment modelled with the sections of 0 to 2 and the venturi wedge opened.

4.2 Residual results

The figures presented in this chapter are a collection of all results standard deviation plotted against the mean value of percentage EGR. The idea is to prove differences between the models depending on EGR percentage.

First the Figures 4.9 and 4.10 are plotted with the modelled value from section 0 to section 2 with opened or closed venturi wedge for all three models.

As the two previous figures the next two Figure 4.11 and 4.12 are the results to prove that the model can be used to model from sections 0 to * with opened or closed venturi wedge.

Figure 4.13 and 4.14 are the result with both opened and closed venturi wedge of the modelled value from sections 0 to 2 and from sections 0 to *. What is important in these figures are how the models behave comparing to percentage EGR and not how the different settings on the venturi wedge change the result.

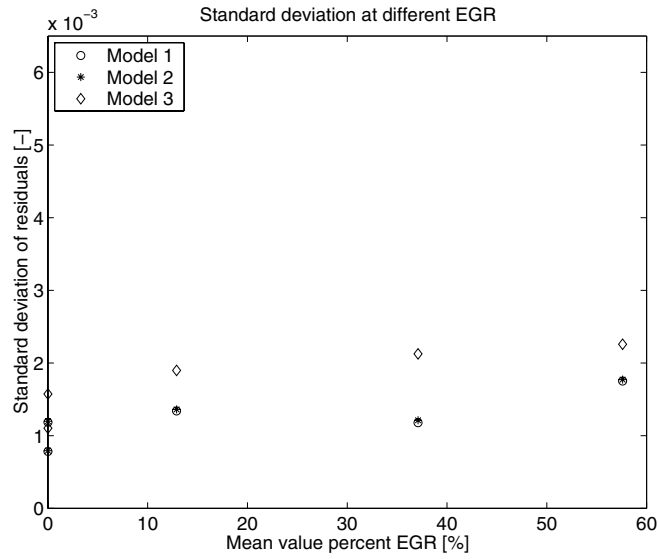


Figure 4.10: Standard deviation of the residuals from experiment modelled 0 to 2 and closed wedge.

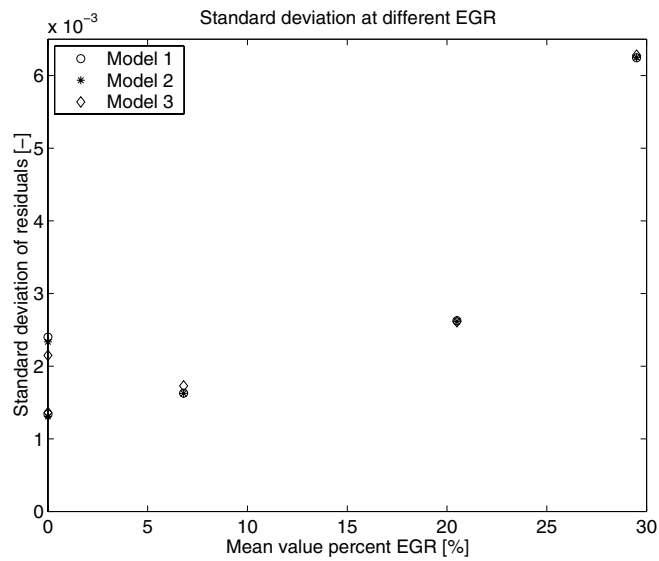


Figure 4.11: Standard deviation of the residuals from experiment modelled 0 to * and opened wedge.

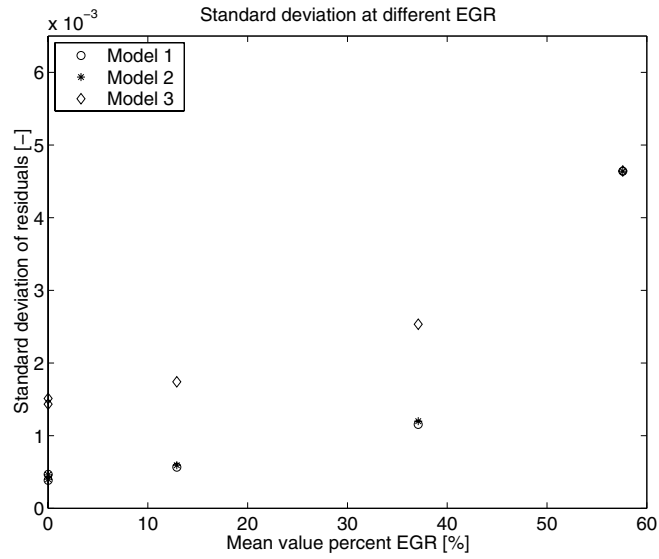


Figure 4.12: Standard deviation of the residuals from experiment modelled 0 to * and closed wedge.

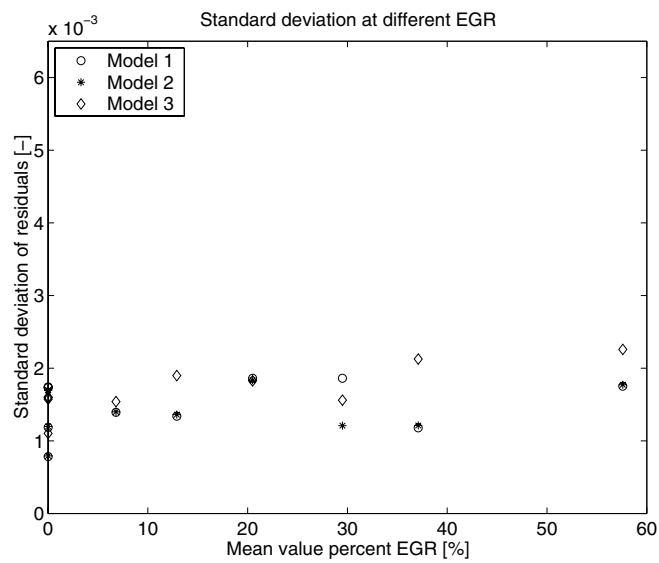


Figure 4.13: Standard deviation of the residuals from both experiment modelled 0 to 2, opened and closed wedge.

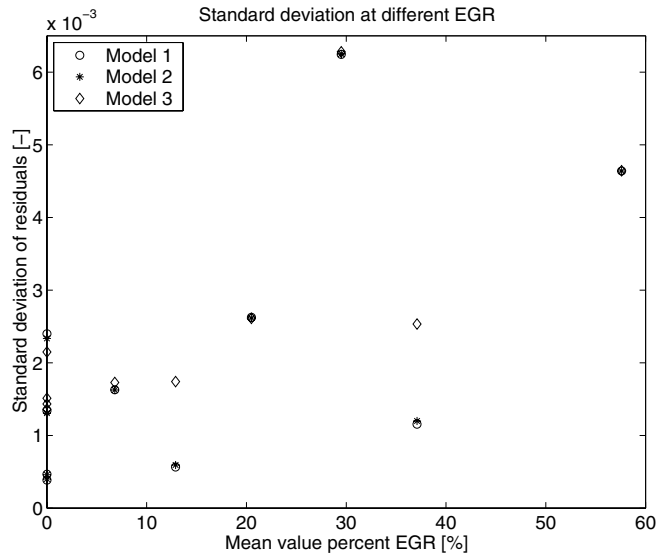


Figure 4.14: Standard deviation of the residuals from both experiment modelled 0 to *, opened and closed wedge.

4.3 Air velocity

The different air velocities calculated through the venturi is at section 0, * and 2. The interesting velocity is at the throat but as the mass flow of EGR is neglected the velocity of the sum of the two flows can not be calculated correct. The focus of the velocity before the venturi w_0 is therefore given or else no comparison would be made correct.

Noticeable in Figure 4.15 and 4.16 are the differences in velocities. The maximum velocity difference is, for the same percentage EGR with only the venturi wedge opened or closed, $w_{\text{closed}} - w_{\text{opened}} = 198.2 - 110.8 = 87.4 \text{ m/s}$ or $w_{\text{closed}}/w_{\text{opened}} = 198.2/110.8 = 1.79$.

4.4 Discussion

One way to verify the models mass flow is to plot it against the measured mass flow. A straight line represent that the modelled mass flow is corresponding to the measured mass flow. The standard deviation is calculated from the residual of the estimated mass flow and the measured mass flow. Another way used to verify the model is if the straight line intersect the origin.

When analyzing the different models and comparing each model

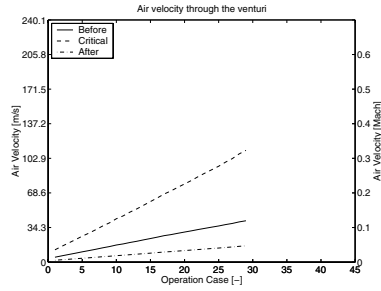


Figure 4.15: Velocities through the venturi in experiment with minimum EGR and *opened* venturi wedge.

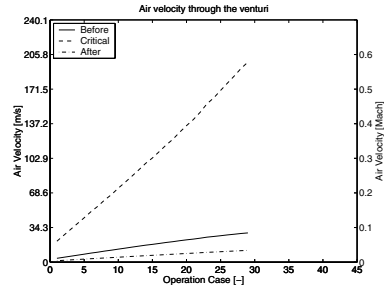


Figure 4.16: Velocities through the venturi in experiment with minimum EGR and *closed* venturi wedge.

with the other, the comparison is what differs between the assumptions. From Sections 2.3, 2.4 and 2.5 the differences of assumptions is

1. the speed before the venturi, w_0 is neglected in model 2 and model 3,
2. in model 3 the flow is assumed to be incompressible which is not the case for model 1 and model 2.

However, from theory about incompressible and compressible flow the magnitude of the velocity of the air is of importance. The velocity differs by a factor of ~ 2 in some experiments if the venturi wedge is opened or closed as seen in Section 3.4. Comparing results from experiments made with opened and closed wedge should be made with caution due to the change from incompressible to compressible flow.

4.4.1 Venturi model 1

When modelling from section 0 to 2 the discharge coefficient decrease when higher percentage EGR is introduced. The model's result, the straight line crosses the x-axis closer to the origin when using opened venturi wedge.

From section 0 to * the discharge coefficient change the opposite way and increase when percentage EGR is increased.

The standard deviation is higher in all experiments for model 1 when using opened venturi wedge with one exception, maximum EGR and opened venturi wedge when modelling from section 0 to 2.

4.4.2 Venturi model 2

As previous, when modelling the model 1, the discharge coefficient change in the same way. It decreases when modelling from 0 to 2 and increases from 0 to *.

The standard deviation behaves in the same manner as for the model 1. For experiments with opened wedge it is higher and less correct. Model 1 has got 11 lower standard deviation out of 20.

As for the intersection of the models result as the straight line it crosses the x-axis closer to the origin more often when using opened wedge. Model 1 intersect closer to the origin 19 times out of 20.

4.4.3 Venturi model 3

The model 3 discharge coefficient decreases with higher percentage EGR when modelling from section 0 to 2 and increases when modelling from 0 to *.

As the other two models, when modelling with opened venturi wedge, the intersection of the x-axis and the straight line, representing model 3, is closer to origin and thus a better fit. Model 1 intersect closer to the origin in all experiments.

As for the standard deviation, model 1 shows 15 better results out of 20 in the different experiments.

4.4.4 Residual results

The residual results from experiments with opened venturi wedge, Figure 4.9 and Figure 4.11, illustrates that there is little differences between the models for each EGR percentage. One data quantity differs though. The highest EGR percentage in Figure 4.9.

Model 3 has got a less good fit than model 1 and 2 in experiments with the venturi wedge closed, Figure 4.10 and Figure 4.12, with one exception for the last data in Figure 4.12.

A relation depending on percent EGR and fit of the models when modelling between section 0 and * could not be found. The amplitude of standard deviation is increasing, as seen in Figure 4.14. However, the amplitude of the standard deviation is increasing and worsening within each experiment when modelling from section 0 to * as illustrated in Figure 4.11 and Figure 4.12.

Higher percentage EGR is achieved with lower pressure in the critical section, the venturi throat. Lower pressure is achieved with greater velocity of the medium, the air passing the throat. When closing the venturi wedge the area in the throat is reduced. Equation 2.3 gives that a constant mass flow \dot{m} and a reduced area A must increase the

product ρw . The density at the given section is when the temperature is constant $\rho = \rho(p_*)$ and the pressure will decrease and w_* must increase. Consequently, experiments with closed venturi wedge leads to greater velocities, Figure 4.15 and Figure 4.16. Model 3 assume incompressible flow. At higher velocities, with closed venturi wedge, the flow is not incompressible and therefor shows less good fit than model 1 and 2. Velocities of air through an engine at full load is compressible and therefore model 3 is rejected, Figure 3.2.

4.4.5 Discharge coefficient

The discharge coefficient, C_D change with different percentage EGR. It is not a function of only percent EGR or velocity of air. Due to the fact, that if it was a function of velocity, then it would not increase with percentage EGR. The maximum velocity in the different experiments are almost the same, therefore it can not be depending on velocities alone.

The coefficient also changes with different models for the same experiment. It is a complex coefficient and not a constant.

One suggestion might be that the flow of EGR is some sort of resistance against the mass flow through the venturi, when trying to approximate the mass flow through the venturi with the pressure in the throat. In the case when modelling from section 0 to 2 it makes it easier for the flow, when increasing percentage EGR, and the coefficient decreases. In the other case the coefficient increases when modelling from section 0 to * for increasing mass flow EGR.

Chapter 5

Conclusions and extensions

An attempt has been made to present a model of a variable venturi that can be used to model the mass flow through the EGR and secondly, verify how the same model approximates the mass flow through the whole variable venturi, from section 0 to 2.

5.1 Conclusions

If different models can approximate the pressure of the different sections in the variable venturi, the mass flow in that section can also be approximated.

Three models with different simplifications have been compared. The assumptions that vary between the models are that model 2 does not take the initial velocity into account but model 1 does. What differs between model 2 and model 3 is, that model 3 further assumes incompressible air flow.

It is shown that model 3 approximates the mass flow through the venturi worse, in the experiments, than the other two models for increasing velocities as the venturi wedge is closed. In an engine even higher velocities are reached and therefore model 3 is not recommended for modelling the venturi and the mass flow of EGR.

Model 1 has got the best fit of the three and the straight line representing model 1 cuts the x-axis closer to the origin than the other two models. However, model 1 is the most complex model of the three and requires more calculations to approximate the mass flow of EGR and therefore takes more time to calculate. If model accuracy is more important than the time it takes to calculate the mass flow, model 1

is recommended otherwise model 2, if time to approximate is more critical.

As model 2 approximates the air velocity before the venturi to zero, in a real engine when velocities are higher, the approximation can worsen the result of the model 2.

5.2 Extensions

Possible future work with the model of a variable venturi.

Discharge coefficient The discharge coefficient should be examined further. If an equation for the real air flow losses and resistance can be found, the models approximation would be better.

Real engine experiments The models should be tried with a real engine in both static and dynamic experiments.

Diffusor separation The theory of air flow in a divergent channel discusses the problem of separation. Does the variable venturi have problems with separation and does increasing EGR flow enhance the problem.

EGR mass flow The three models presented in this thesis assume the mass flow of EGR to be very small and therefore neglected. Investigate how the model works with the mass flow of EGR included. Since the temperature of the EGR gases is higher, the energy of EGR mass flow should be considered.

References

- [1] Scania World Wide Web. About us. <http://www.scania.com/au/>, September 2002.
- [2] Marshall Brain. How Diesel Engines Work. <http://www.howstuffworks.com/diesel.htm>, November 2002.
- [3] John B. Heywood. *Internal combustion engine fundamentals*. Mechanical engineering series. McGraw-Hill, Singapore, international edition edition, 1988.
- [4] Ingvar Ekroth and Eric Granryd. *Tillämpad termodynamik*. Institutionen för Energiteknik, Avdelningen för Tillämpad termodynamik och kylteknik, Kungliga Tekniska Högskolan, Stockholm, Sweden, 1994. In Swedish.
- [5] Frank W. Schmidt, Robert E. Henderson, and Carl H. Wolgemuth. *Introduction to thermal sciences: thermodynamics, fluid dynamics, heat transfer*. John Wiley & Sons, Inc, New York, USA, second edition edition, 1993.
- [6] Scania CV. Henrik Höglund, NMEE. Experiment engine data. Internal document, Scania., March 2002.
- [7] Scania CV. S. Ryhänen. Sensor temp/pressure tab dwg. specification for sensor with cable and connector. Internal document, Scania., March 2002. Part no. 1399310.
- [8] BOSCH. Technical customer information. Calibration data sheet, March 1995. BOSCH Product part no. 0 280 217 119, Prod. type HFM2C.
- [9] Karl Storck, Matts Karlsson, and Dan Loyd. Formelsamling i strömningslära, termodynamik och värmeöverföring. Technical Report LiTH-IKP-S-424, Mekanisk värmeteori och strömningslära, Institutionen för Konstruktions- och Produktionsteknik, Linköping, Sweden, November 1996. Course material, Linköpings Universitet, Sweden.

Notation

Symbols used in the report. Symbols index is set corresponding to the real engine sensor or engine part placement.

Variables and parameters

A	Area	m^2
C_D	Discharge coefficient	—
c_p	Specific heat at constant pressure	$J/kg \cdot K$
c_v	Specific heat at constant pressure	$J/kg \cdot K$
\dot{E}	Rate of energy transfer as work	W
ε	Work	Nm/kg
g	Gravitational acceleration	m/s^2
h	Enthalpy	J/kg
κ	Ratio of specific heats, quota c_p/c_v	—
\dot{m}	Mass flow rate	kg/s
p	Pressure	Pa
\dot{Q}	Heat transfer	J/s
ρ	Density	kg/m^3
T	Temperature	K
v	Specific volume	m^3/kg
w	Velocity	m/s
z	Height	m

Appendix A

Equations

Derivations of general equations used in this thesis is made in this appendix.

A.1 General equations

The derivation made is to help understand simpler equation manipulation and the equations used is defined in [5], [4] and [9]. In the Chapter 5.2, notation is found and is used instead of the literatures definitions.

Density is defined as

$$v = \frac{1}{\rho}. \quad (\text{A.1})$$

Assume isentropic process, then

$$pv^\kappa = \text{const}. \quad (\text{A.2})$$

Ideal gas law is

$$pv = RT. \quad (\text{A.3})$$

A.2 Derivations

Use new indexes as $\alpha = 0$ and $\beta = *$ from Figure 2.1 and (A.2) then

$$p_\alpha v_\alpha^\kappa = p_\beta v_\beta^\kappa \quad (\text{A.4})$$

and solve for v_α together with (A.3) is

$$v_\alpha = \left(\frac{p_\beta}{p_\alpha}\right)^{\frac{1}{\kappa}} v_\beta = \left(\frac{p_\beta}{p_\alpha}\right)^{\frac{1}{\kappa}} \frac{RT_\beta}{p_\beta}. \quad (\text{A.5})$$

Use definition of density, (A.1) then

$$\rho_\alpha = \left(\frac{p_\beta}{p_\alpha}\right)^{-\frac{1}{\kappa}} \frac{p_\beta}{RT_\beta} \quad (\text{A.6})$$

and the product of densities are

$$\frac{\rho_\alpha}{\rho_\beta} = \frac{v_\beta}{v_\alpha} = \left(\frac{p_\alpha}{p_\beta}\right)^{\frac{1}{\kappa}}. \quad (\text{A.7})$$

A more specific derivation of $\frac{T_\beta}{T_\alpha} = \left(\frac{p_\beta}{p_\alpha}\right)$ from Section 2.3 and (2.8).
As previous use new indexes α and β then

$$(T_\alpha - T_\beta) = T_\alpha \left(1 - \frac{T_\beta}{T_\alpha}\right) \quad (\text{A.8})$$

together with (A.4) and (A.3) is

$$p_\beta \left(\frac{RT_\beta}{p_\beta}\right)^\kappa = p_\alpha \left(\frac{RT_\alpha}{p_\alpha}\right)^\kappa. \quad (\text{A.9})$$

A rewriting and division gives

$$\left(\frac{T_\beta}{T_\alpha}\right)^\kappa = \frac{p_\alpha}{p_\beta} \left(\frac{p_\beta}{p_\alpha}\right)^\kappa \quad (\text{A.10})$$

and finally

$$\frac{T_\beta}{T_\alpha} = \left(\frac{p_\alpha}{p_\beta}\right)^{\frac{1}{\kappa}} \left(\frac{p_\alpha}{p_\beta}\right)^{-\frac{\kappa}{\kappa}} = \left(\frac{p_\beta}{p_\alpha}\right)^{\frac{\kappa-1}{\kappa}}. \quad (\text{A.11})$$

Appendix B

Results

The most part of the plots from results and experiment are found in this appendix.

B.1 Velocities through the venturi

Presented here is the velocities through the venturi. Theory of calculations is founded in Chapter 3.4.

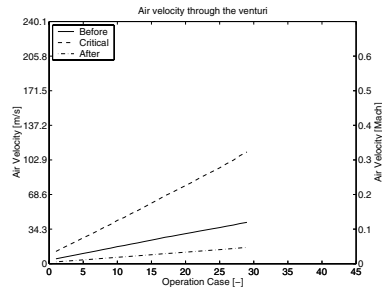


Figure B.1: Velocities through the venturi in experiment with minimum EGR and opened venturi wedge.

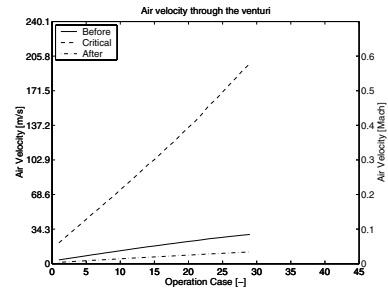


Figure B.2: Velocities through the venturi in experiment with minimum EGR and closed venturi wedge.

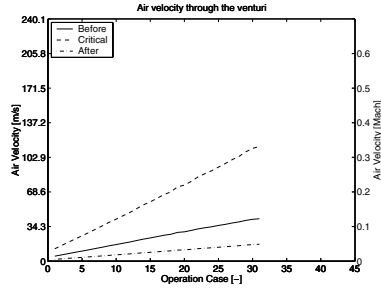


Figure B.3: Velocities through the venturi in experiment with low EGR and opened venturi wedge.

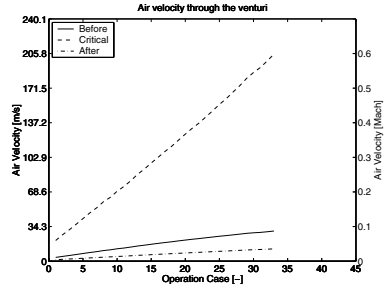


Figure B.4: Velocities through the venturi in experiment with low EGR and closed venturi wedge.

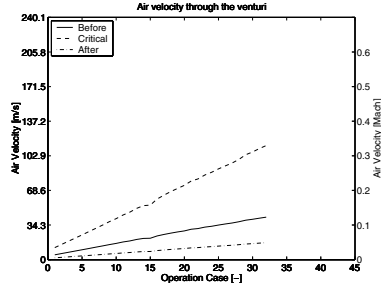


Figure B.5: Velocities through the venturi in experiment with medium EGR and opened venturi wedge.

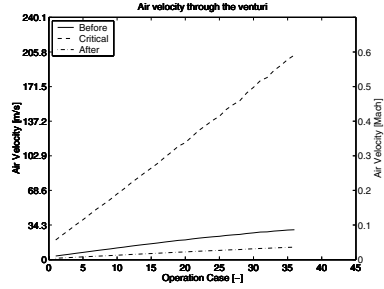


Figure B.6: Velocities through the venturi in experiment with medium EGR and closed venturi wedge.

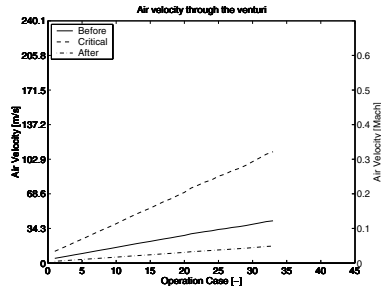


Figure B.7: Velocities through the venturi in experiment with high EGR and opened venturi wedge.

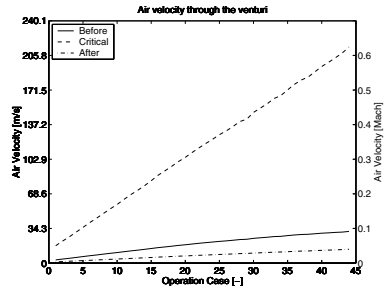


Figure B.8: Velocities through the venturi in experiment with high EGR and closed venturi wedge.

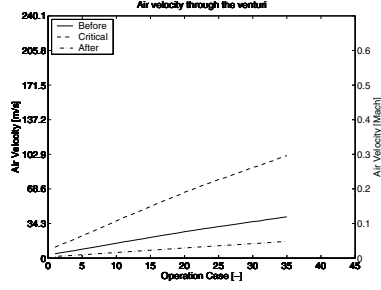


Figure B.9: Velocities through the venturi in experiment with maximum EGR and opened venturi wedge.

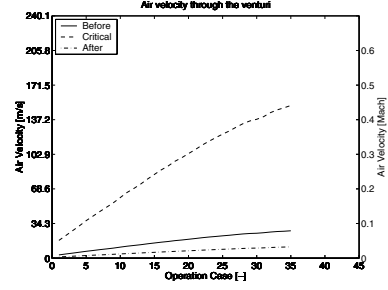


Figure B.10: Velocities through the venturi in experiment with maximum EGR and closed venturi wedge.

Table B.1: Maximum velocities at different sections in the venturi in experiment with opened wedge.

Experiment	Before	Critical	After
Minimum	41.0	110.8	16.2
Low	42.0	113.7	16.7
Medium	42.1	113.0	16.8
High	41.9	110.3	16.8
Maximum	41.0	101.6	16.6

Table B.2: Maximum velocities at different sections in the venturi in experiment with closed wedge.

Experiment	Before	Critical	After
Minimum	29.0	198.2	11.6
Low	29.9	205.3	12.2
Medium	29.6	202.8	12.3
High	31.3	214.2	13.7
Maximum	27.1	151.3	11.2

B.2 Venturi model 1

The result in this section, mostly from Chapter 4, are approximated with the model 1, found in Section 2.3. First the ten model fitting from section 0 to 2 in the venturi and lower in this section the ten model fittings from section 0 to *. After each section, the tables is to be found and in them the standard deviation from the different fittings.

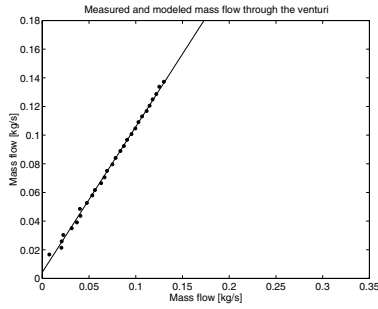


Figure B.11: Model 1 from section 0 to 2 with minimum EGR and opened venturi wedge.

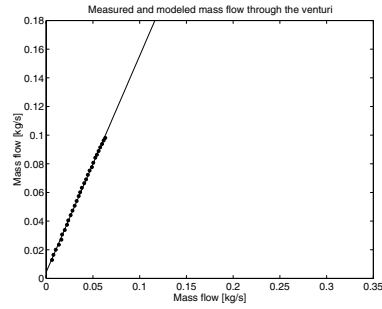


Figure B.12: Model 1 from section 0 to 2 with minimum EGR and closed venturi wedge.

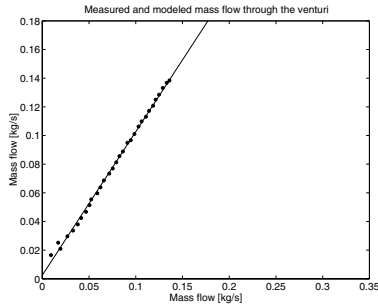


Figure B.13: Model 1 from section 0 to 2 with low EGR and opened venturi wedge.

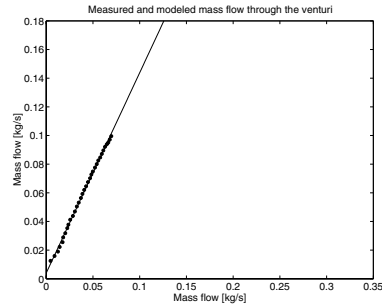


Figure B.14: Model 1 from section 0 to 2 with low EGR and closed venturi wedge.

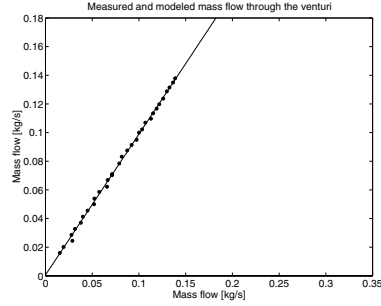


Figure B.15: Model 1 from section 0 to 2 with medium EGR and opened venturi wedge.

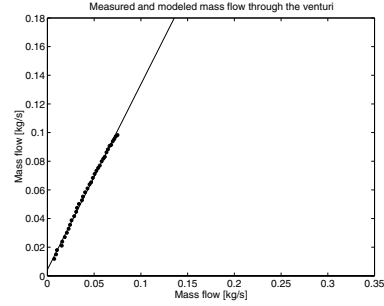


Figure B.16: Model 1 from section 0 to 2 with medium EGR and closed venturi wedge.

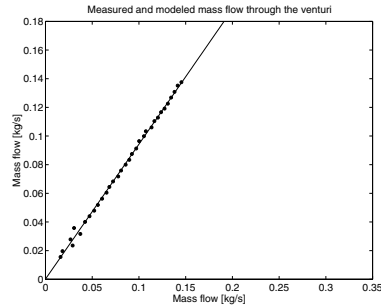


Figure B.17: Model 1 from section 0 to 2 with high EGR and opened venturi wedge.

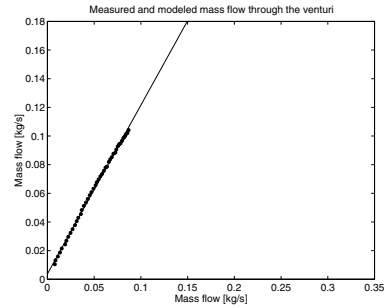


Figure B.18: Model 1 from section 0 to 2 with high EGR and closed venturi wedge.

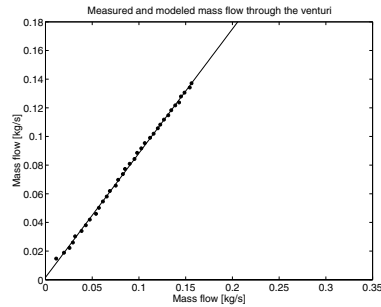


Figure B.19: Model 1 from section 0 to 2 with maximum EGR and opened venturi wedge.

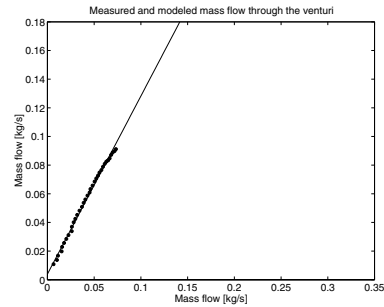


Figure B.20: Model 1 from section 0 to 2 with maximum EGR and closed venturi wedge.

Table B.3: Results of fittings. Model 1, section 0 to 2.

Experiment	Coefficients, p1	Coefficients, p2	Norm of residuals	Standard deviation
Minimum opened	1.0157	0.0042773	0.0093283	1.732e-003
Low opened	1.0017	0.0024589	0.0097047	1.743e-003
Medium opened	0.98349	0.00056242	0.0078713	1.391e-003
High opened	0.94146	0.00012837	0.010691	1.861e-003
Maximum opened	0.86695	0.0016089	0.0069057	1.167e-003

Table B.4: Results of fittings. Model 1, section 0 to 2.

Experiment	Coefficients, p1	Coefficients, p2	Norm of residuals	Standard deviation
Minimum closed	1.51	0.0043754	0.004211	0.782e-003
Low closed	1.3984	0.0039437	0.006802	1.184e-003
Medium closed	1.2937	0.0043287	0.0080386	1.340e-003
High closed	1.1781	0.0037128	0.0078101	1.177e-003
Maximum closed	1.2429	0.0038986	0.010366	1.752e-003

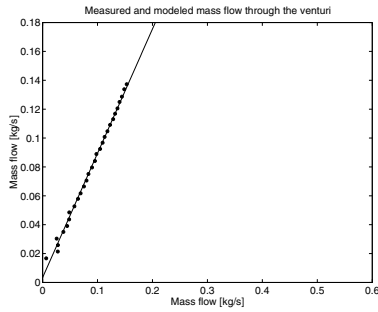


Figure B.21: Model 1 from section 0 to * with minimum EGR and opened venturi wedge.

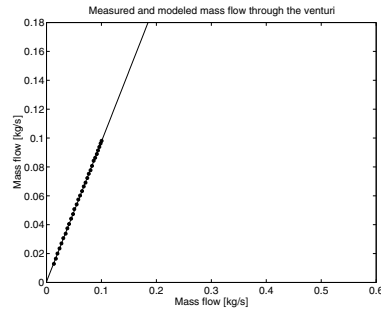


Figure B.22: Model 1 from section 0 to * with minimum EGR and closed venturi wedge.

Table B.5: Results of fittings. Model 1, section 0 to *.

Experiment	Coefficients, p1	Coefficients, p2	Norm of residuals	Standard deviation
Minimum opened	0.86123	0.0032745	0.012919	2.399e-003
Low opened	0.90807	0.0010207	0.0074619	1.340e-003
Medium opened	0.9388	0.00026054	0.0092119	1.628e-003
High opened	1.0925	-0.00028319	0.015077	2.625e-003
Maximum opened	2.1275	-0.00079254	0.036941	6.244e-003

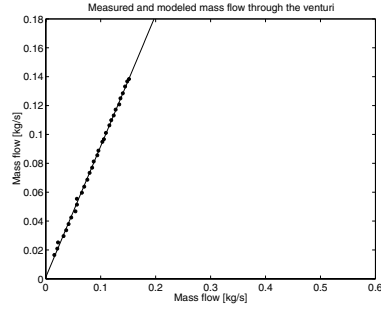


Figure B.23: Model 1 from section 0 to * with low EGR and opened venturi wedge.

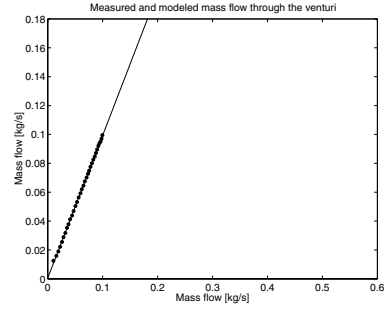


Figure B.24: Model 1 from section 0 to * with low EGR and closed venturi wedge.

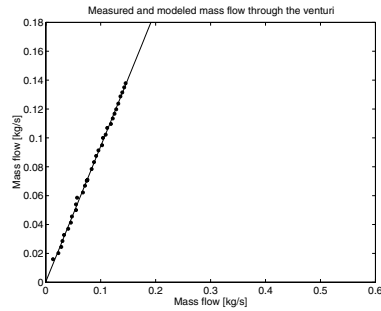


Figure B.25: Model 1 from section 0 to * with medium EGR and opened venturi wedge.

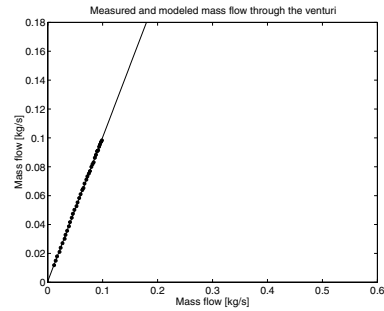


Figure B.26: Model 1 from section 0 to * with medium EGR and closed venturi wedge.

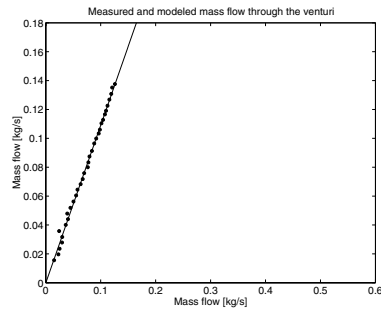


Figure B.27: Model 1 from section 0 to * with high EGR and opened venturi wedge.

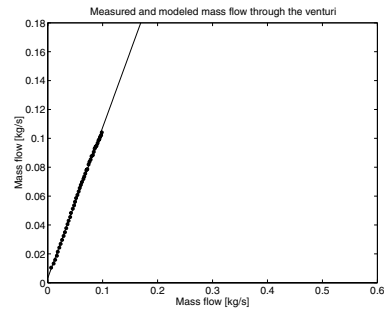


Figure B.28: Model 1 from section 0 to * with high EGR and closed venturi wedge.

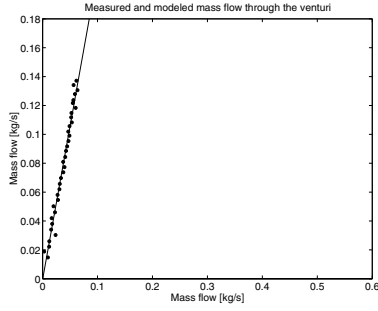


Figure B.29: Model 1 from section 0 to * with maximum EGR and opened venturi wedge.

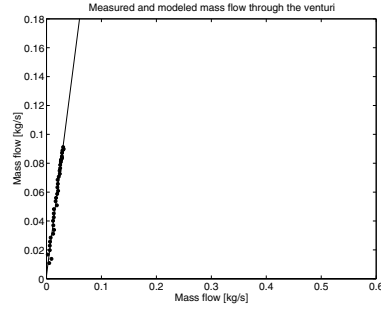


Figure B.30: Model 1 from section 0 to * with maximum EGR and closed venturi wedge.

Table B.6: Results of fittings. Model 1, section 0 to *.

Experiment	Coefficients, p1	Coefficients, p2	Norm of residuals	Standard deviation
Minimum closed	0.97117	0.00046634	0.0020747	0.385e-003
Low closed	0.98886	0.00038561	0.0026826	0.467e-003
Medium closed	0.99858	0.00054486	0.0033943	0.566e-003
High closed	1.0447	0.0030482	0.007653	1.154e-003
Maximum closed	2.9585	0.0021822	0.027442	4.639e-003

B.3 Venturi model 2

The result in this section, mostly from Chapter 4, are approximated with the model 2, found in Section 2.4. First the ten model fitting from section 0 to 2 in the venturi and lower in this section the ten model fittings from section 0 to *. After each section, the tables is to be found and in them the standard deviation from the different fittings.

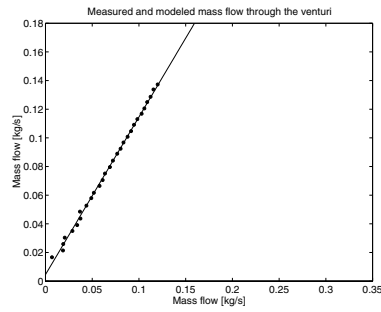


Figure B.31: Model 2 from section 0 to 2 with minimum EGR and opened venturi wedge.

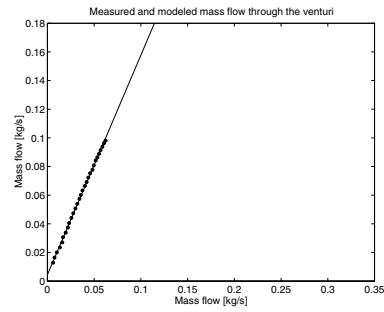


Figure B.32: Model 2 from section 0 to 2 with minimum EGR and closed venturi wedge.

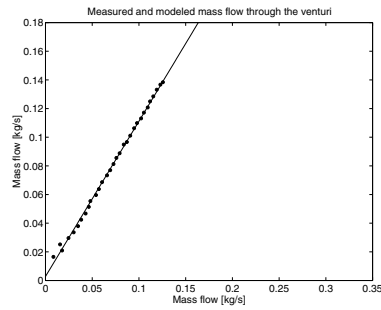


Figure B.33: Model 2 from section 0 to 2 with low EGR and opened venturi wedge.

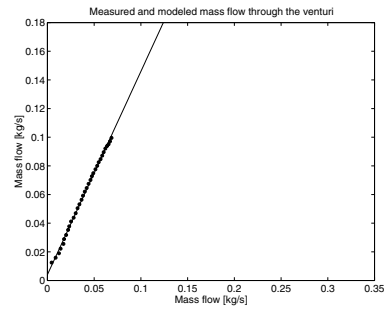


Figure B.34: Model 2 from section 0 to 2 with low EGR and closed venturi wedge.

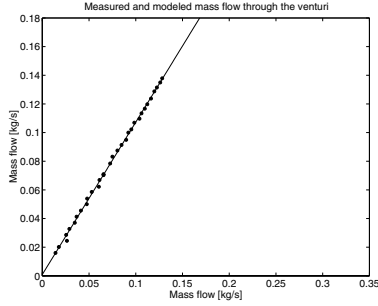


Figure B.35: Model 2 from section 0 to 2 with medium EGR and opened venturi wedge.

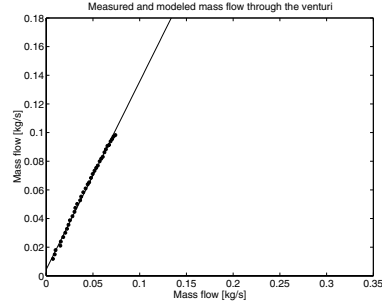


Figure B.36: Model 2 from section 0 to 2 with medium EGR and closed venturi wedge.

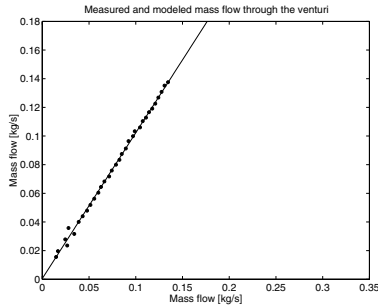


Figure B.37: Model 2 from section 0 to 2 with high EGR and opened venturi wedge.

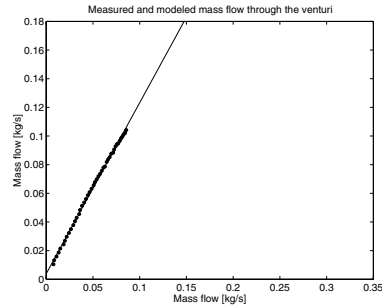


Figure B.38: Model 2 from section 0 to 2 with high EGR and closed venturi wedge.

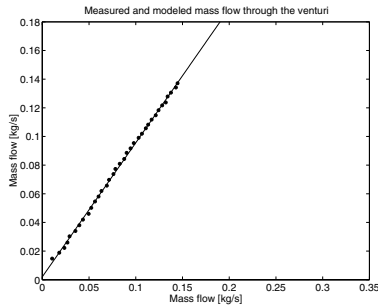


Figure B.39: Model 2 from section 0 to 2 with maximum EGR and opened venturi wedge.

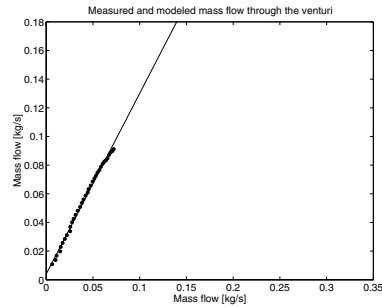


Figure B.40: Model 2 from section 0 to 2 with maximum EGR and closed venturi wedge.

Table B.7: Results of fittings. Model 2, section 0 to 2.

Experiment	Coefficients, p1	Coefficients, p2	Norm of residuals	Standard deviation
Minimum opened	1.1002	0.0045204	0.0091285	1.695e-003
Low opened	1.0839	0.0027552	0.0094432	1.696e-003
Medium opened	1.0633	0.00090573	0.0079153	1.399e-003
High opened	1.0173	0.0004886	0.01053	1.833e-003
Maximum opened	0.93566	0.0020095	0.007152	1.209e-003

Table B.8: Results of fittings. Model 2, section 0 to 2.

Experiment	Coefficients, p1	Coefficients, p2	Norm of residuals	Standard deviation
Minimum closed	1.533	0.00442	0.0042731	0.793e-003
Low closed	1.419	0.0040029	0.0068785	1.197e-003
Medium closed	1.3123	0.0043982	0.0081649	1.361e-003
High closed	1.1939	0.0038134	0.008042	1.212e-003
Maximum closed	1.2609	0.0039609	0.010483	1.772e-003

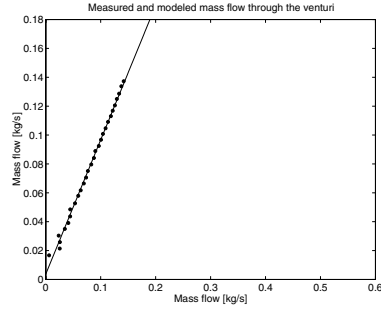


Figure B.41: Model 2 from section 0 to * with minimum EGR and opened venturi wedge.

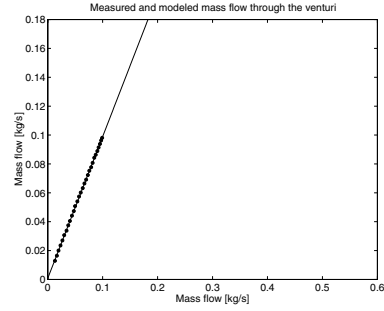


Figure B.42: Model 2 from section 0 to * with minimum EGR and closed venturi wedge.

Table B.9: Results of fittings. Model 2, section 0 to *.

Experiment	Coefficients, p1	Coefficients, p2	Norm of residuals	Standard deviation
Minimum opened	0.93018	0.0036246	0.012568	2.334e-003
Low opened	0.98031	0.0014211	0.0072757	1.307e-003
Medium opened	1.0141	0.00064106	0.0091906	1.625e-003
High opened	1.1833	-1.1933e-005	0.015025	2.616e-003
Maximum opened	2.3237	-0.00084934	0.036982	6.251e-003

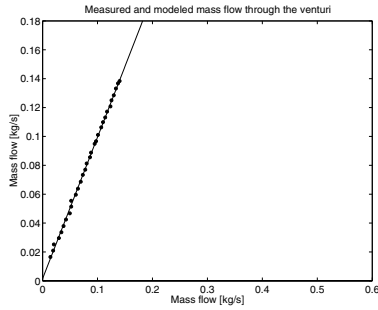


Figure B.43: Model 2 from section 0 to * with low EGR and opened venturi wedge.

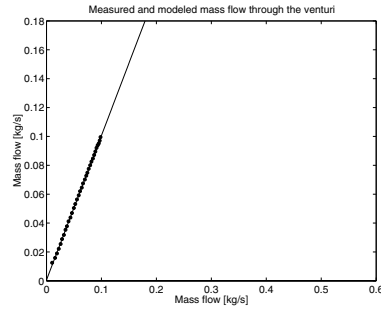


Figure B.44: Model 2 from section 0 to * with low EGR and closed venturi wedge.

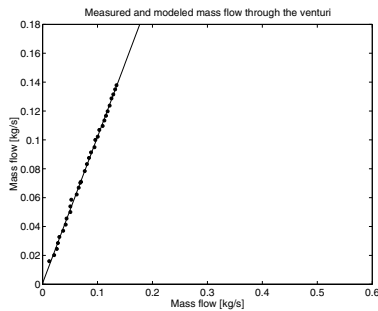


Figure B.45: Model 2 from section 0 to * with medium EGR and opened venturi wedge.

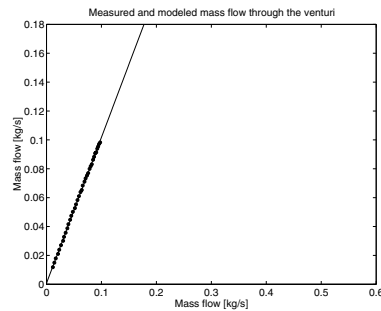


Figure B.46: Model 2 from section 0 to * with medium EGR and closed venturi wedge.

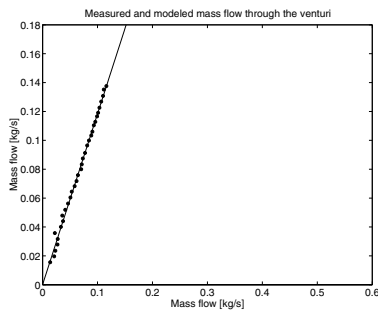


Figure B.47: Model 2 from section 0 to * with high EGR and opened venturi wedge.

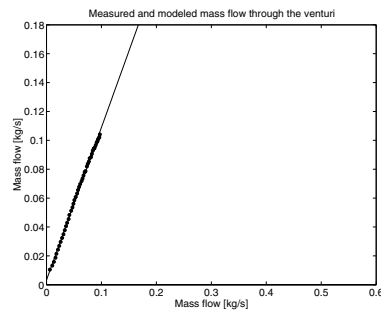


Figure B.48: Model 2 from section 0 to * with high EGR and closed venturi wedge.

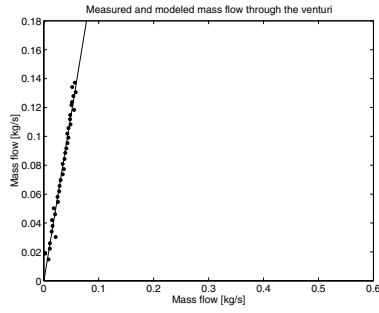


Figure B.49: Model 2 from section 0 to * with maximum EGR and opened venturi wedge.

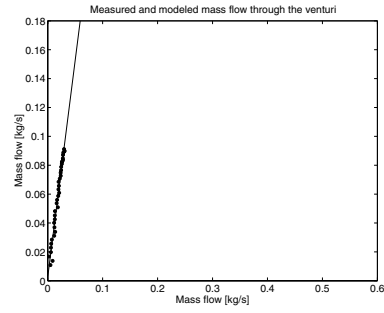


Figure B.50: Model 2 from section 0 to * with maximum EGR and closed venturi wedge.

Table B.10: Results of fittings. Model 2, section 0 to *.

Experiment	Coefficients, p1	Coefficients, p2	Norm of residuals	Standard deviation
Minimum closed	0.98272	0.00061447	0.0021616	0.401e-003
Low closed	1.0006	0.0005359	0.0026446	0.460e-003
Medium closed	1.0105	0.0006923	0.0035588	0.593e-003
High closed	1.0574	0.0031875	0.0079571	1.200e-003
Maximum closed	3.0073	0.0021925	0.027442	4.639e-003

B.4 Venturi model 3

The result in this section, mostly from Chapter 4, are approximated with the model 3, found in Section 2.5. First the ten model fitting from section 0 to 2 in the venturi and lower in this section the ten model fittings from section 0 to *. After each section, the tables is to be found and in them the standard deviation from the different fittings.

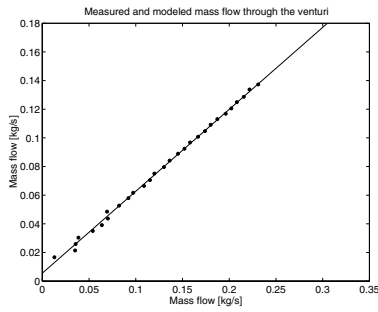


Figure B.51: Model 3 from section 0 to 2 with minimum EGR and opened venturi wedge.

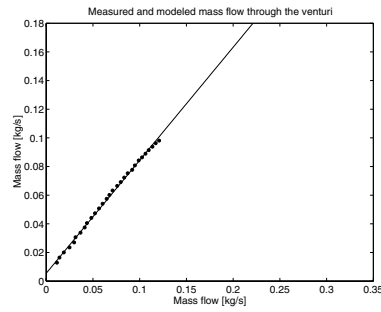


Figure B.52: Model 3 from section 0 to 2 with minimum EGR and closed venturi wedge.

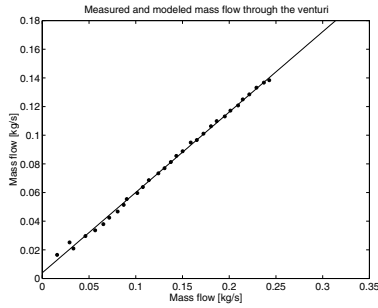


Figure B.53: Model 3 from section 0 to 2 with low EGR and opened venturi wedge.

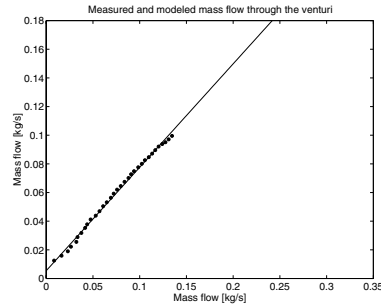


Figure B.54: Model 3 from section 0 to 2 with low EGR and closed venturi wedge.

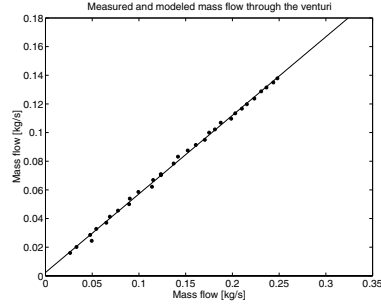


Figure B.55: Model 3 from section 0 to 2 with medium EGR and opened venturi wedge.

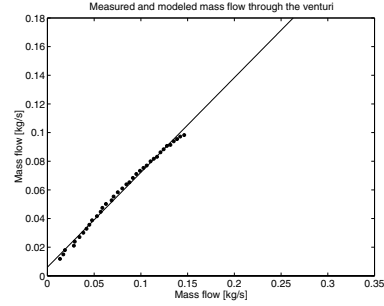


Figure B.56: Model 3 from section 0 to 2 with medium EGR and closed venturi wedge.

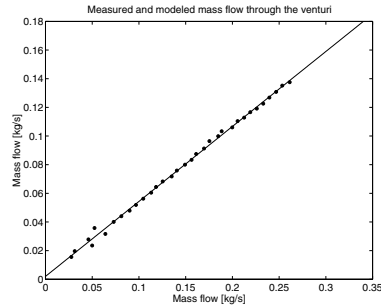


Figure B.57: Model 3 from section 0 to 2 with high EGR and opened venturi wedge.

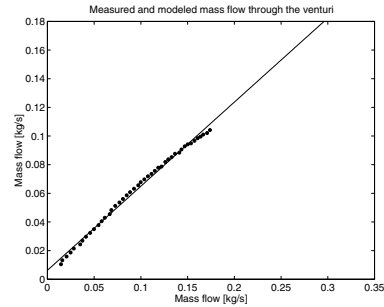


Figure B.58: Model 3 from section 0 to 2 with high EGR and closed venturi wedge.

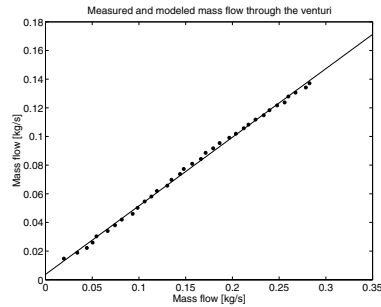


Figure B.59: Model 3 from section 0 to 2 with maximum EGR and opened venturi wedge.

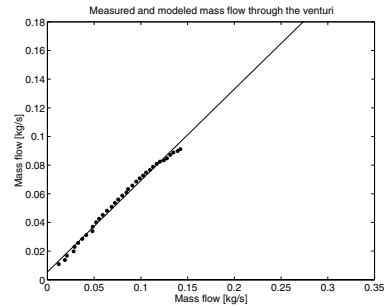


Figure B.60: Model 3 from section 0 to 2 with maximum EGR and closed venturi wedge.

Table B.11: Results of fittings. Model 3, section 0 to 2.

Experiment	Coefficients, p1	Coefficients, p2	Norm of residuals	Standard deviation
Minimum opened	0.5719	0.0055211	0.0086246	1.602e-003
Low opened	0.56082	0.0039839	0.0088636	1.592e-003
Medium opened	0.54839	0.0023265	0.0087078	1.539e-003
High opened	0.52329	0.0019884	0.010483	1.825e-003
Maximum opened	0.47868	0.0036913	0.0092218	1.559e-003

Table B.12: Results of fittings. Model 3, section 0 to 2.

Experiment	Coefficients, p1	Coefficients, p2	Norm of residuals	Standard deviation
Minimum closed	0.78889	0.0054472	0.0059359	1.102e-003
Low closed	0.72203	0.0053824	0.0090343	1.573e-003
Medium closed	0.66148	0.0060333	0.011385	1.898e-003
High closed	0.58691	0.0062552	0.014101	2.126e-003
Maximum closed	0.63802	0.0054187	0.013357	2.258e-003

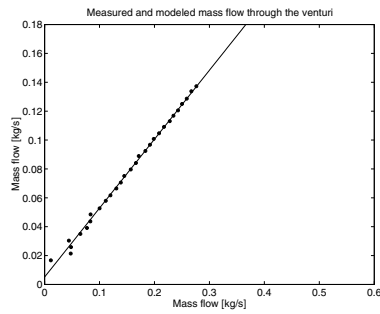


Figure B.61: Model 3 from section 0 to * with minimum EGR and opened venturi wedge.

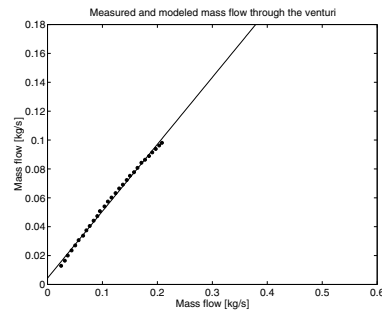


Figure B.62: Model 3 from section 0 to * with minimum EGR and closed venturi wedge.

Table B.13: Results of fittings. Model 3, section 0 to *.

Experiment	Coefficients, p1	Coefficients, p2	Norm of residuals	Standard deviation
Minimum opened	0.47744	0.0050921	0.011572	2.149e-003
Low opened	0.50215	0.0030975	0.007586	1.362e-003
Medium opened	0.52091	0.0022236	0.0097796	1.729e-003
High opened	0.61495	0.0010989	0.015005	2.612e-003
Maximum opened	1.2496	-0.0010725	0.037151	6.280e-003

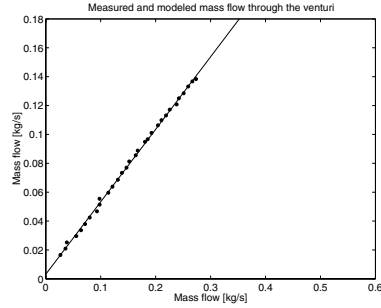


Figure B.63: Model 3 from section 0 to * with low EGR and opened venturi wedge.

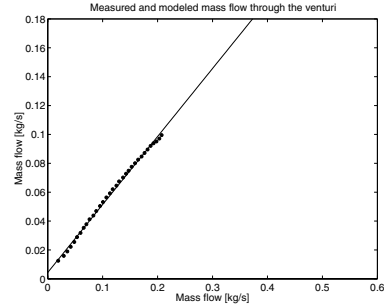


Figure B.64: Model 3 from section 0 to * with low EGR and closed venturi wedge.

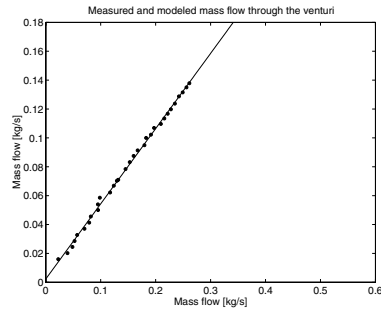


Figure B.65: Model 3 from section 0 to * with medium EGR and opened venturi wedge.

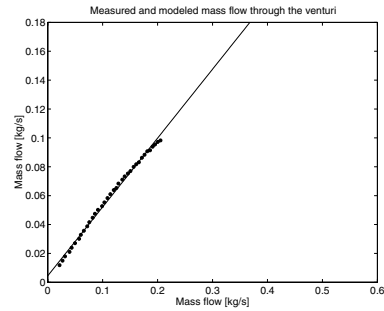


Figure B.66: Model 3 from section 0 to * with medium EGR and closed venturi wedge.

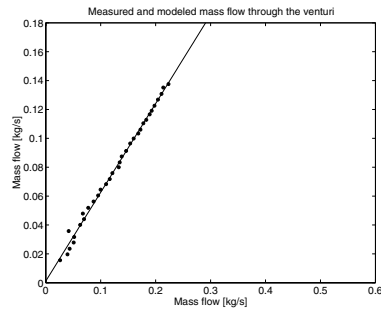


Figure B.67: Model 3 from section 0 to * with high EGR and opened venturi wedge.

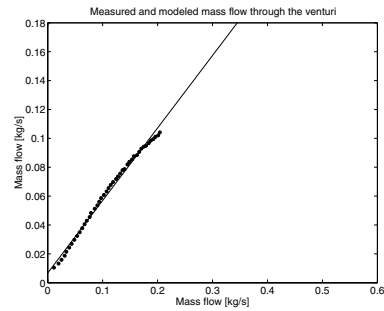


Figure B.68: Model 3 from section 0 to * with high EGR and closed venturi wedge.

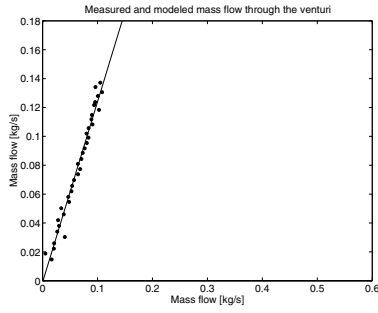


Figure B.69: Model 3 from section 0 to * with maximum EGR and opened venturi wedge.

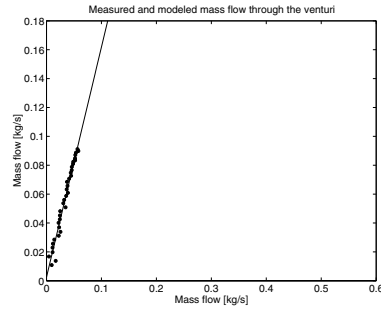


Figure B.70: Model 3 from section 0 to * with maximum EGR and closed venturi wedge.

Table B.14: Results of fittings. Model 3, section 0 to *.

Experiment	Coefficients, p1	Coefficients, p2	Norm of residuals	Standard deviation
Minimum closed	0.46362	0.0043302	0.00814	1.512e-003
Low closed	0.47109	0.0043279	0.0082298	1.433e-003
Medium closed	0.4772	0.0043963	0.010448	1.741e-003
High closed	0.50221	0.0067124	0.016805	2.533e-003
Maximum closed	1.5937	0.0024221	0.027461	4.642e-003